

University of Wollongong  
**Research Online**

---

Faculty of Science, Medicine and Health -  
Papers: part A

Faculty of Science, Medicine and Health

---

1-1-2014

**Very long hillslope transport timescales determined from uranium-series isotopes in river sediments from a large, tectonically stable catchment**

P O. Suresh

*Macquarie University*, [suresh.puthiyaveetil-othayoth@mq.edu.au](mailto:suresh.puthiyaveetil-othayoth@mq.edu.au)

Anthony Dosseto

*University of Wollongong*, [tonyd@uow.edu.au](mailto:tonyd@uow.edu.au)

Paul P. Hesse

*Macquarie University*

Heather K. Handley

*Macquarie University*

Follow this and additional works at: <https://ro.uow.edu.au/smhpapers>



Part of the [Medicine and Health Sciences Commons](#), and the [Social and Behavioral Sciences Commons](#)

---

**Recommended Citation**

Suresh, P O.; Dosseto, Anthony; Hesse, Paul P.; and Handley, Heather K., "Very long hillslope transport timescales determined from uranium-series isotopes in river sediments from a large, tectonically stable catchment" (2014). *Faculty of Science, Medicine and Health - Papers: part A*. 2629.

<https://ro.uow.edu.au/smhpapers/2629>

Research Online is the open access institutional repository for the University of Wollongong. For further information contact the UOW Library: [research-pubs@uow.edu.au](mailto:research-pubs@uow.edu.au)

---

## Very long hillslope transport timescales determined from uranium-series isotopes in river sediments from a large, tectonically stable catchment

### Abstract

The uranium-series isotopic compositions of soils and sediments evolve in response to time and weathering conditions. Therefore, these isotopes can be used to constrain the timescales of river sediment transport. Catchment evolution depends on the sediment dynamic timescales, on which erosion imparts a major control. Erosion rates in tectonically stable catchments are expected to be lower than those in tectonically active catchments, implying longer sediment residence times in tectonically stable catchments. Mineralogical, elemental and isotopic data are presented for modern channel sediments, alluvial and colluvial deposits from the Murrumbidgee River, a large catchment in the passive margin highlands of south-eastern Australia and three of its tributaries from the headwaters to the alluvial plain. Low variability in Si-based Weathering Index indicates that there is little chemical weathering occurring in the Murrumbidgee River during sediment transport. However, quartz content increases and plagioclase content decreases downstream, indicating progressive mineralogical sorting and/or physical comminution with increasing transport distance. U-series isotopic ratios in the Murrumbidgee River trunk stream sediments show no systematic downstream variation. The weathering ages of sediments within the catchment were determined using a loss-gain model of U-series isotopes. Modern sediments from a headwater tributary, the Bredbo River at Frogs Hollow, have a weathering age of  $76 \pm 30$  kyr but all other modern channel sediments from the length of the Murrumbidgee River and its main tributaries have weathering ages  $\sim 400 \pm 180$  kyr. The two headwater colluvial deposits have weathering ages of  $57 \pm 13$  and  $47 \pm 11$  kyr, respectively. All the alluvial deposits have weathering ages similar to those of modern sediments. No downstream trend in weathering age is observed. Together with the soil residence time of up to 30 kyr for ridge-top soils at Frogs Hollow in the upper catchment area of the Murrumbidgee River (Suresh et al., 2013), the current results indicate, for the first time, that sediments in the Murrumbidgee catchment are stored in hill slope for long time ( $\sim 200$  kyr) before carried by the river. The long residence times of sediments indicate a low erosion rate from the catchment. The sediment transport timescales estimated are up to two orders of magnitude higher than those reported for tectonically active catchments in Iceland (Vigier et al., 2006) and in the Himalayas (Granet et al., 2007), indicating the influence of tectonism on catchment erosion.

### Disciplines

Medicine and Health Sciences | Social and Behavioral Sciences

### Publication Details

Suresh, P. O., Dosseto, A., Hesse, P. P. & Handley, H. K. (2014). Very long hillslope transport timescales determined from uranium-series isotopes in river sediments from a large, tectonically stable catchment. *Geochimica et Cosmochimica Acta*, 142 442-457.

1 **Very Long Hillslope Transport Timescales Determined from Uranium-**  
2 **Series Isotopes in River Sediments from a Large, Tectonically Stable**  
3 **Catchment**

4

5

6 P. O. Suresh<sup>1\*</sup>, A. Dosseto<sup>2</sup>, P. P. Hesse<sup>1</sup> and H. K. Handley<sup>3</sup>

7 <sup>1</sup>Department of Environment and Geography, Macquarie University, Sydney, Australia

8 <sup>2</sup>Wollongong Isotope Geochronology Laboratory, School of Earth and Environmental Sciences, University of  
9 Wollongong, Australia

10 <sup>3</sup>GEMOC, Department of Earth and Planetary Sciences, Macquarie University, Sydney, Australia

11

12

13

14

15

16

17

18

19

20

21 \*Corresponding author

22 Department of Environment and Geography, Macquarie University, Sydney NSW 2109, Australia. E-  
23 mail: [suresh.puthiyaveetil- othayoth@mq.edu.au](mailto:suresh.puthiyaveetil-othayoth@mq.edu.au).

24 Current address

25 R & D Division, Gujarat State Fertilizers and Chemicals Limited, Fertilizer Nagar, Vadodara, Gujarat –  
26 391750, India. Email: [posuresh@gsfcltd.com](mailto:posuresh@gsfcltd.com). Phone: +91-2653092529. Fax: +91-2652240966

28 **Abstract**

29 The uranium-series isotopic compositions of soils and sediments evolve in response to time  
30 and weathering conditions. Therefore, these isotopes can be used to constrain the timescales  
31 of river sediment transport. Catchment evolution depends on the sediment dynamic  
32 timescales, on which erosion imparts a major control. Erosion rates in tectonically stable  
33 catchments are expected to be lower than those in tectonically active catchments, implying  
34 larger sediment residence times in tectonically stable catchments. Mineralogical, elemental  
35 and isotopic data are presented for modern channel sediments, alluvial and colluvial deposits  
36 from the Murrumbidgee River, a large catchment in the passive margin highlands of south-  
37 eastern Australia and three of its tributaries from the headwaters to the alluvial plain. Low  
38 variability in Si-based Weathering Index indicates that there is little chemical weathering  
39 occurring in the Murrumbidgee River during sediment transport. However, quartz content  
40 increases and plagioclase content decreases downstream, indicating progressive  
41 mineralogical sorting and/or physical comminution with increasing transport distance. U-  
42 series isotopic ratios in the Murrumbidgee River trunk stream sediments show no systematic  
43 downstream variation. The weathering ages of sediments within the catchment were  
44 determined using a loss-gain model of U-series isotopes. Modern sediments from a headwater  
45 tributary, the Bredbo River at Frogs Hollow, have a weathering age of  $76 \pm 30$  kyr but all  
46 other modern channel sediments from the length of the Murrumbidgee River and its main  
47 tributaries have weathering ages  $\sim 400 \pm 180$  kyr. The two headwater colluvial deposits have  
48 weathering ages of  $57 \pm 13$  and  $47 \pm 11$  kyr, respectively. All the alluvial deposits have  
49 weathering ages similar to those of modern sediments. No downstream trend in weathering  
50 age is observed. Together with the soil residence time of up to 30 kyr for ridge-top soils at  
51 Frogs Hollow in the upper catchment area of the Murrumbidgee River (Suresh et al., 2013),  
52 the current results indicate, for the first time, that sediments in the Murrumbidgee catchment  
53 are stored in hill slope for long time ( $\sim 200$  kyr) before carried by the river. The long  
54 residence times of sediments indicate a low erosion rate from the catchment. The sediment  
55 transport timescales estimated are up to two orders of magnitude higher than those reported  
56 for tectonically active catchments in Iceland (Vigier et al., 2006) and in the Himalayas  
57 (Granet et al., 2007), indicating the influence of seismicity on catchment erosion.

58

59 **Keywords**

60 Murrumbidgee River, U-series isotopes, sediment residence time, alluvium, weathering age

61

62 **1. Introduction**

63 The evolution of uranium-series (U-series) activity ratios during weathering is  
64 affected by factors such as pH, the presence of organic matter, and time. U-series isotopes are  
65 expected to be in secular equilibrium (parent-daughter activity ratio = 1) in unweathered  
66 bedrock older than 1 Myr (Bourdon et al., 2003; Dosseto et al., 2008a). If the half-life of the  
67 parent isotope is longer than the daughter isotope, then in a period of ~5 half-lives of the  
68 daughter nuclide, the parent daughter activity ratio will reach secular equilibrium (Bourdon et  
69 al., 2003) (half-lives of  $^{238}\text{U}$ ,  $^{234}\text{U}$  and  $^{230}\text{Th}$  are  $4.4683 \times 10^9$  years (Jaffey et al., 1971),  
70  $24.525 \times 10^4$  years and  $75.69 \times 10^3$  years (Cheng et al., 2000), respectively). Fractionation  
71 between isotopes during geological processes such as chemical weathering induces  
72 radioactive disequilibrium. During chemical weathering, U is preferentially mobilized over  
73 Th (Chabaux et al., 2003). Oxidizing conditions prevail in most weathering environments and  
74 so U will be present as  $\text{U}^{6+}$ , which is soluble in waters as the uranyl ion,  $\text{U}_{\text{VI}}\text{O}_2^{2+}$  and is  
75 stabilized by highly soluble and non-reactive carbonate complexes (Langmuir, 1978). Th will  
76 be present as  $\text{Th}^{4+}$ , which is insoluble. This causes elemental fractionation between U and Th,  
77 and affects the ( $^{230}\text{Th}/^{234}\text{U}$ ) activity ratios of weathered material. In addition, the high energy  
78 involved in the radioactive decay of U-series isotopes can damage crystal lattices and  
79 enhance loss of the daughter nuclide by leaching from damaged recoil tracks, hence creating  
80 disequilibrium in the parent-daughter activity ratio (Kigoshi, 1971, Rosholt, 1983, Chabaux  
81 et al., 2003, Vigier et al., 2011). Also, if radioactive decay occurs near the surface of the grain  
82 a fraction of the daughter nuclide may be directly ejected from a mineral grain (Kigoshi,  
83 1971; DePaolo et al., 2006). The degree of fractionation of U-series isotopes in soils and  
84 sediments can be used to determine the timescale of weathering and erosion processes, as the  
85 radioactive disequilibrium is time dependent.

86 Soil residence time (Table 1) and production rates have been determined in different  
87 climatic and geomorphic settings through modelling the evolution of uranium-series isotopes

88 in soil (Mathieu et al., 1995; Dequincey et al., 2002; Dosseto et al., 2008b; Ma et al., 2010;  
89 Dosseto et al., 2012; Suresh et al., 2013). Using the same model, the weathering age (Table  
90 1) of sediments transported by rivers in a variety of geographical locations and climatic  
91 settings have been determined by Vigier et al. (2001; 2005; 2006), Dosseto et al. (2006a; b,  
92 2008b) and Granet et al. (2007; 2010). Variations are observed in calculated sediment  
93 weathering ages between catchments and are controlled by changes in climate, human  
94 activity, relief, tectonic activity and bedrock composition.

95         The dissolved and suspended loads of sediments in rivers largely show shorter  
96 transport timescales (a few kyr) (Dosseto et al., 2008b, Granet et al., 2010) relative to the  
97 coarser particle load, such as the bedload (in the order of ~100 kyr or more) (Dosseto et al.,  
98 2008b, Granet et al., 2010). Suspended sediments from tropical rivers flowing through  
99 basaltic terrain in the Deccan Traps have given residence times 55 – 84 kyr (Vigier et al.,  
100 2005), whereas those from rivers draining basaltic terrain in Iceland gave residence times 1 –  
101 8 kyr (Vigier et al., 2006). The two order of magnitude difference in residence times of  
102 sediments from lowland Amazon Rivers (100 – 500 kyr) and upland Amazon Rivers (3 – 4  
103 kyr) could be due to differences in catchment relief in the two regions (Dosseto et al., 2006a,  
104 b). Suspended sediments from the upper Ganga (Ganges) River and tributaries in the  
105 Himalayas gave residence times ~30 kyr, but those from the river on the Ganga plain showed  
106 much higher residence times (~350 kyr) (Granet et al., 2007). The longer residence times on  
107 the alluvial plains may be due to reworking of old sediments in the plain. Lower relief  
108 compared to the upper river basin in the plain could also imply slower transport. In summary,  
109 large variations in sediment residence times in rivers are observed showing the influence of  
110 different factors like climate, catchment geomorphology and glaciation, controlling sediment  
111 movements in the catchment areas. Studying the sediment transport timescales and the  
112 affecting factors in the Murrumbidgee catchment, a tectonically stable passive margin in the  
113 highland area of south-eastern Australia where periglacial conditions prevailed during the  
114 Last Glacial Maximum (LGM), will further our current understanding of soil and landscape  
115 evolution in large catchments. A consolidated study of sediments in alluvium, colluviums  
116 and modern channel is expected to provide new insights on their evolution throughout the  
117 catchment.

118         Soil processes in the upper Murrumbidgee catchment are affected by factors such as  
119 rainfall and topography (Suresh et al., 2013). Ridge-top soil residence times of approximately

120 30 kyr have been determined using U-Th isotopes in the upper catchment area of the  
121 Murrumbidgee River (Suresh et al., 2013). Heimsath et al. (2001) reported soil production  
122 rate of ~ 45 mm/kyr by measuring cosmogenic radionuclides of  $^{26}\text{Al}$  and  $^{10}\text{Be}$  concentrations  
123 in soils at this location. Using this rate, Yoo et al. (2007) estimated a lateral transport time of  
124 ~60 kyr for soils along a 50 m hillslope profile. Dosseto et al. (2010) estimated comminution  
125 ages (Table 1) of  $\leq 50 \mu\text{m}$  size sediments from palaeochannels and the modern channel of the  
126 Murrumbidgee River. They reported comminution ages an order of magnitude lower for the  
127 post-Last Glacial Maximum (LGM) sediments than the Holocene and pre-LGM sediments.  
128 The authors attributed the lower sediment residence time (Table 1) of the post-LGM  
129 sediments to the erosion of materials from the upper catchment and the higher sediment  
130 residence time of the modern and pre-LGM sediments to the reworking of alluvial deposits.

131 This paper presents U-series isotope, mineralogical and major element data of modern  
132 sediments, alluvial and colluvial deposits from the Murrumbidgee River of south-eastern  
133 Australia. The data are used to estimate the weathering ages of sediments in the catchment. In  
134 combination with the soil residence times determined using U-series isotopes (Suresh et al.,  
135 2013) and long-term erosion rates determined using cosmogenic radionuclides (Fujioka et al.,  
136 2012), the data are used to constrain the timescales of sediment dynamics from initial  
137 weathering to final deposition in this large catchment. This will aid our understanding of the  
138 long-term evolution and sustainability of landscapes in large catchments. The proposed  
139 change in sediment source, pre- and post-LGM, in the Murrumbidgee catchment described by  
140 Dosseto et al. (2010) is also re-examined using the new results.

141

## 142 **2. Study Area**

143 The Murrumbidgee River in south-eastern Australia is divided into three distinct  
144 geomorphic regions (Wallbrink et al., 1998). The upper catchment is a mountainous region  
145 with high relief (up to 2000 m above sea level) comprising an area of approximately 20,500  
146  $\text{km}^2$  (Fig. 1). Burrinjuck Dam isolates the upper from the middle Murrumbidgee catchment  
147 (combined area 34,000  $\text{km}^2$ ). The middle catchment is characterized by rolling terrain with  
148 gullying (Wallbrink et al., 1998) and progressively decreasing tributary input to the river  
149 further downstream. The river enters the lower Murrumbidgee alluvial plain downstream of  
150 Narrandera to eventually merge with the Murray River. Average annual rainfall in the

151 catchment area ranges from 1900 mm in the upper mountains to less than 350 mm on the  
152 plain (NSW Water, 2011).

153 Modern sediment samples (currently being transported by the river) were collected  
154 from riverbanks and bars at 7 locations throughout the length of the Murrumbidgee River, in  
155 the section between the confluence of the Bredbo River with the Murrumbidgee River in the  
156 mountainous, bedrock-confined upper catchment and Darlington Point in the alluvial plain  
157 (Fig. 1). These modern samples were either deposited or mobilized by recent flows. Modern  
158 channel sediments were collected above and below the confluences of the river with major  
159 tributaries, namely the Bredbo, Goodradigbee and the Tumut Rivers. A modern sediment  
160 sample from the upper Bredbo River was collected from Frogs Hollow, ~40 km upstream of  
161 Bredbo (Fig. 1). Alluvial deposits from four locations along the Murrumbidgee River were  
162 sampled at different depths, wherever possible (Table 2). These samples, from deep bank  
163 exposures, represent older and/or higher floodplain deposits of likely Holocene age. Two  
164 samples from the alluvial deposits at Wangrah Creek, a minor tributary in the upper  
165 catchment (studied by Prosser et al., 1994) area also were collected. Two colluvial deposit  
166 samples were collected from a gully near Bredbo. The colluvial sediments were deposited by  
167 runoff and sheetwash processes at the base of a ridge. A late Pleistocene dust deposit sample  
168 (deposition age =  $21.6 \pm 2$  ka, determined by optically stimulated luminescence dating; in  
169 Fitzsimmons et al. 2013) was collected at a depth of 150 cm from McKenzie's Waterhole  
170 Creek near Carcoar (Fig. 1; Hesse et al. 2003), to assess the contribution of aeolian material  
171 to the U-series isotope composition of river sediments.

172

### 173 **3. Materials and Method**

174 Modern sediments were collected from banks and bars of the river channel. Colluvial  
175 and alluvial deposits were sampled from natural bank exposures adjacent to the channel. The  
176 depositional ages of alluvial sediments are unknown, except for those from Wangrah Creek  
177 (MU8\_low and up,  $12,420 \pm 150$  yr BP; radiocarbon age; Prosser et al., 1994).

178 All of the samples were dried at 60°C overnight. Aliquots of each sample were placed  
179 in acid-cleaned polypropylene containers for X-ray diffraction (XRD), X-ray fluorescence  
180 (XRF) and U-series isotopic analysis.



181 Dried samples were powdered to ~10 µm size for XRD using an agate mortar and  
182 pestle. X-ray diffractograms were recorded using a PANalytical X'pert PRO MPD  
183 diffractometer with a 45 kV, 40 mA CuKα radiation X'celerator detector and Bragg Brentano  
184 geometry, conducting scans from 5 to 50° 2θ at 5° 2θ/min. Highscore Plus software version  
185 2.2.4 with the ICDD PDF2 database by PANalytical and the basic Rietveld refinement option  
186 available in the software were used for mineral identification and quantification, respectively.

187 Sediment aliquots for major element analysis were powdered to less than 10 µm and  
188 prepared into 40 mm glass discs by fusion with lithium borate containing lanthanum oxide  
189 (Norrish and Hutton, 1969). Analyses were performed using a Philips PW2400 XRF  
190 instrument at Mark Wainwright Analytical Centre (University of New South Wales),  
191 following the procedure described by Norrish and Hutton (1969). Reproducibility of the  
192 results was determined by replicate sample analysis (3 samples) yielding an elemental oxide  
193 standard error below 1 % for all elements.

194 For U-series analysis, samples were ashed at 550 °C overnight. Approximately 2 g of  
195 ashed sample was leached with Mg(NO<sub>3</sub>)<sub>2</sub> to remove ion exchangeable uranium and thorium  
196 from the grain surfaces and U-Th bound to the organic matter destroyed during ashing  
197 (Gleyzes et al., 2002). Approximately 100 mg of leached sample was weighed into 15 ml  
198 PFA vials and approximately 30 mg of a <sup>236</sup>U-<sup>229</sup>Th tracer solution was added and weighed.  
199 The samples were then digested in a mixture of HCl, HNO<sub>3</sub>, HF and HClO<sub>4</sub> in closed vials at  
200 120 °C overnight. The sample solutions were then dried and then redissolved in 7M HNO<sub>3</sub>. U  
201 and Th were separated and purified using an anion exchange resin (Biorad AG1X8)  
202 following a procedure described in Sims et al. (2008). Measurement of U and Th isotopes  
203 were performed on a Nu Instruments Nu-Plasma multi-collector ICPMS instrument following  
204 the procedure outlined in Turner et al. (2011). Reproducibility of the results was assessed by  
205 replicating the whole procedure for two samples. This yielded a reproducibility of 0.17 % for  
206 Th concentration, 0.8 % for U concentration, 1.2 % for (<sup>234</sup>U/<sup>238</sup>U) and 3 % for (<sup>230</sup>Th/<sup>238</sup>U).  
207 Accuracy was determined by measuring the U-series isotopic ratios and U-Th concentrations  
208 in TML-3, a standard rock sample (Table Mountain Latite, Williams et al., 1992; Sims et al.,  
209 2008). The measured concentrations and activity ratios are within 2σ error limits of published  
210 values (Table 2; Sims et al., 2008). The total procedural blank was 150 pg for U and 140 pg  
211 for Th, which are insignificant when compared to the U and Th amounts of sediment samples  
212 digested (~0.5 µg of U and ~2.5 µg of Th for 0.1g of sample).

213

## 214 **4. Results**

### 215 *4.1. Mineralogy*

216 All of the modern channel sediment samples contain > 60 wt. % quartz, except for the  
217 sample from the Bredbo River at Frogs Hollow (Table 3; Fig. 2). Albite, microcline and  
218 muscovite contents vary from 0 to 20 wt. %. Illite was detected only in some of the modern  
219 sediments (Table 3). All the alluvial deposit samples except MU8\_up contain > 60 wt. %  
220 quartz (Table 3). Albite content varies from 0 to 20 wt. %, microcline from 0 to 10 wt. % and  
221 muscovite from 3 to 54 wt. %. Illite was detected only in the alluvial sample collected from  
222 Darlington Point (1.6 wt. %). Colluvial deposit samples contain 61 wt. % quartz and  
223 approximately 30 wt. % muscovite. Albite was detected (6 wt. %) in only one of the colluvial  
224 samples (Table 3). XRD analysis detected only quartz in the dust sample.

225

### 226 *4.2. Particle size*

227 All the modern sediment samples, except MU11 from the Bredbo River at Frogs  
228 Hollow, contain > 25 % mud (Table 3). Alluvial samples contain variable proportions of mud  
229 (< 63 µm) and sand (63 to 2,000 µm) (Table 3). The alluvial deposit sample MU3 from the  
230 deposits near the Bredbo – Murrumbidgee confluence is the coarsest, with only 2 % mud.  
231 The alluvial samples from a single deposit contain variable proportions of mud at different  
232 depth. For example, the sample MU8\_up from 1.4 m depth at Wangrah Creek contains 74 %  
233 mud, whereas the sample MU8\_low from 3.6 m depth contains 37 % mud. These variations  
234 reflect the mixed suspended (mud) and bed (sand) load nature of the Murrumbidgee River  
235 and reflect small variations of depositional environment within the river bed and proximal  
236 floodplain.

237

### 238 *4.3. Major Elements*

239 Major element data are given in Table S1 in the Appendix. All of the samples contain  
240 > 64 wt. % SiO<sub>2</sub>, except sample MU8\_up from the Wangrah Creek alluvial deposit, with 57

241 wt. % SiO<sub>2</sub>. Greater than 10 wt. % Al<sub>2</sub>O<sub>3</sub>, ~ 2 to 9 wt. % Fe<sub>2</sub>O<sub>3</sub> and > 2 wt. % K<sub>2</sub>O were  
242 detected in all samples. An increase in SiO<sub>2</sub> and decrease in Al<sub>2</sub>O<sub>3</sub> with decreasing depth is  
243 observed for alluvial deposits at Gundagai and colluvial samples from Bredbo gully. The dust  
244 sample contains 84 wt. % SiO<sub>2</sub>, 6 wt. % Al<sub>2</sub>O<sub>3</sub> and 4 wt. % Fe<sub>2</sub>O<sub>3</sub> (Table S1).

245

#### 246 *4.4. U-series isotopes*

247 U concentrations in the samples range from 1.7 to 6.3 ppm and Th concentrations  
248 vary between 9.6 and 21.8 ppm in alluvial deposits (Table 2). The highest U and Th  
249 concentrations were observed in the alluvial samples MU8\_up from Wangrah Creek and  
250 MU19\_low from Gundagai. In alluvial deposits from Gundagai, U and Th concentrations  
251 decrease with decreasing depth. The two colluvial samples from Bredbo have nearly identical  
252 U and Th concentrations. For the modern sediment samples, U and Th concentrations display  
253 a range similar to those of alluvial deposits.

254 All of the sediment samples have (<sup>234</sup>U/<sup>238</sup>U) activity ratios greater than 1, indicating  
255 the relative enrichment of <sup>234</sup>U. The ratios vary from 1.02 to 1.35 in the alluvial deposits and  
256 from 1.09 to 1.26 in the modern sediments (Table 2, Fig. 3). All of the sediment samples  
257 except MU3, MU11 and MU22 have (<sup>230</sup>Th/<sup>234</sup>U) ratios lower than 1, varying from 0.61 to  
258 0.86. This also may correspond to enrichment of <sup>234</sup>U.

259 The dust sample contains 11.6 ppm Th and 1.7 ppm U (Table 1). It has a (<sup>234</sup>U/<sup>238</sup>U)  
260 ratio of 0.996 and (<sup>230</sup>Th/<sup>234</sup>U) ratio of 1.24 (Table 2).

261

## 262 **5. Discussion**

### 263 *5.1. Mineral sorting and weathering*

264 The presence of quartz, albite, microcline and muscovite in all sediments is consistent  
265 with the large area of granitic bedrock in the Murrumbidgee catchment. Quartz content  
266 increases and plagioclase content decreases downstream in the modern sediments (Fig. 2).  
267 This could be due either to chemical dissolution of plagioclase, preferential physical  
268 weathering of plagioclase over quartz, or due to mineral hydrodynamic sorting. The lack of

269 evidence for chemical dissolution or physical breakdown (detailed below) of minerals points  
270 towards mineral sorting during river transport. The increasing extent of mineral dissolution  
271 with increasing stream length should correspond to a similar trend in weathering indices,  
272 which is not observed here. The Si-based weathering index ( $WIS = \frac{SiO_2}{(SiO_2+Al_2O_3+CaO+Na_2O)} \times 100$ ) does not show a downstream increasing trend. The  
273 WIS is preferable to other indices of chemical weathering, such as the CIA or CIW (Harnois,  
274 1988) because of the mobilization of Al during weathering in the soil profiles (Driscoll et al.,  
275 1985; White et al., 2008; Suresh et al. 2013; Suresh et al., submitted). The CIA and CIW  
276 indices consider Al to be immobile (Nesbitt and Young, 1982; Harnois, 1988). Suresh et al.  
277 (2013) reported mobility of Al in the soil of the Murrumbidgee catchment. The lack of a  
278 systematic downstream evolution of WIS values either in modern sediments or alluvial  
279 deposits of the Murrumbidgee River suggests that little chemical weathering occurs during  
280 sediment transport (Fig. 4). Physical breakdown of particles or progressive abrasion  
281 downstream should correspond to a decreasing trend in particle size distribution, which is not  
282 observed here (Table 3). Hydrodynamic sorting of minerals, which occurs depending on the  
283 settling velocity of minerals grains (related to their size, density and shape) and flow velocity,  
284 could have affected the distribution of the minerals in the sediments. Observations of mineral  
285 sorting have been reported in the Yamuna River in the Himalayas (Dalai et al., 2004). The  
286 absence of a downstream trend in WIS values may also imply rapid transport of sediments by  
287 the river.  
288

289 Mobilization of elements from sediments has been commonly discussed in  
290 comparison to the composition of the average upper continental crust (UCC) (Taylor and  
291 McLennan, 1985; Dalai et al., 2004). All major element contents were averaged for the  
292 alluvial deposits, modern sediments and colluvium and then normalized to average UCC  
293 contents taken from McLennan (1995) and bedrock values taken from Chappell (1984) (Fig.  
294 5). Normalised Na, Ca and Mg contents are all < 1, indicating loss during chemical  
295 weathering. Al, Si and K are comparatively immobile. Mn seems to be enriched in the  
296 modern and colluvial samples, which could possibly indicate anthropogenic input of Mn, but  
297 the huge error bars limits our ability to draw conclusions (Fig. 5).

298

299 *5.2. Uranium and thorium concentration and activity ratios*

300 U concentrations in the modern channel sediments do not show significant trends with  
301 stream length (Table 2). This may indicate that no significant leaching of U is occurring  
302 during transport. Th concentrations are much more variable than U. Positive correlations  
303 (correlation coefficient  $R = 0.86$  for U and  $0.6$  for Th) exist between sediment mud content  
304 and U and Th concentration (Fig. 6). An increase in soil and sediment U and Th  
305 concentration with decreasing grain size has been reported by Baeza et al. (1995), Lee et al.  
306 (2004) and Suresh et al. (2013). In the modern channel sediment samples, U concentrations  
307 show a strong ( $R = 0.8$ ) positive correlation with muscovite content (Fig. 7). Similar  
308 observations were reported in soil profiles from Frogs Hollow in the catchment area of the  
309 Murrumbidgee River (Suresh et al., 2013). Suresh et al. (2013) proposed that muscovite is the  
310 mineral phase dominating the U budget in the Frogs Hollow soil profiles. Our data suggest  
311 that this is also true in river sediments.

312 The lack of significant chemical weathering during river transport (Fig. 4) could  
313 suggest that there has been little fractionation of U-series isotopes during fluvial transport. A  
314 negative correlation exists between WIS and U and Th concentrations in alluvial or modern  
315 sediments (Fig. 8). These two observations together imply that no significant U or Th loss is  
316 occurring during transport due to chemical weathering. The decrease in U and Th  
317 concentration with increasing WIS may be the result of chemical weathering of sediments  
318 before reaching the river channel. Soils from Frogs Hollow in the upper Murrumbidgee  
319 catchment exhibit WIS values similar to those observed in the river sediments (Fig. 8).

320 ( $^{234}\text{U}/^{238}\text{U}$ ) activity ratios  $> 1$  in all samples suggest an enrichment of  $^{234}\text{U}$  over  $^{238}\text{U}$   
321 (Fig. 3). However, during chemical weathering,  $^{234}\text{U}$  is preferentially removed from the solid  
322 phase, and therefore, ( $^{234}\text{U}/^{238}\text{U}$ )  $< 1$  is expected in the residue of weathering (Chabaux et al.,  
323 2003; Dosseto et al, 2008a). The activity ratio ( $^{234}\text{U}/^{238}\text{U}$ )  $< 1$  is observed in the soil samples  
324 from Frogs Hollow in the upper catchment area of the Murrumbidgee River (Suresh et al.,  
325 2013). This again follows the suggestion that the removal of U and Th from the sediments  
326 occurs before entering in to the river stream. Sediment ( $^{234}\text{U}/^{238}\text{U}$ ) activity ratios  $> 1$  suggest  
327 input of  $^{234}\text{U}$  from a fluid phase. During chemical weathering the  $^{234}\text{U}$  leached from the solid  
328 phase will be concentrated in the fluid, driving the ( $^{234}\text{U}/^{238}\text{U}$ ) ratio in the liquid  $> 1$   
329 (Dequincey et al., 2002; Chabaux et al., 2003; Robinson et al., 2004; Anderson et al., 2007;  
330 2009; Vigier et al., 2011). The mineral phases formed from this fluid are characterised by the  
331 ( $^{234}\text{U}/^{238}\text{U}$ ) ratio of the fluid phase, i.e.  $> 1$  (Plater et al., 1992, Dequincey et al., 2002). The

332  $^{234}\text{U}$  from the fluid phase may be retained by residual phases by several mechanisms  
333 discussed by Scott (1968), namely: 1. Incorporation into the lattices of clay minerals, 2.  
334 Adsorption to mineral surfaces, 3. Association to Al and Fe oxides and 4. Complexation by  
335 organic materials. ( $^{234}\text{U}/^{238}\text{U}$ ) activity ratios  $> 1$  in river sediments have been observed in  
336 Deccan rivers (Vigier et al., 2005), Amazonian rivers (Dosseto et al., 2006a) and Himalayan  
337 rivers (Granet et al., 2007).

338 The ( $^{234}\text{U}/^{238}\text{U}$ ) ratios  $> 1$  and ( $^{230}\text{Th}/^{234}\text{U}$ ) ratios  $< 1$  in sediments imply a net gain of  
339 U over loss to leaching and that the gained U has a higher ( $^{234}\text{U}/^{238}\text{U}$ ) ratio than that in the  
340 leached U component (Dequincey et al., 2002). ( $^{234}\text{U}/^{238}\text{U}$ ) or ( $^{230}\text{Th}/^{234}\text{U}$ ) ratios in the  
341 modern sediments show no systematic downstream evolution. The ( $^{230}\text{Th}/^{234}\text{U}$ ) ratios of all  
342 but two of the modern sediments are similar (averaged at 0.712 with  $1\sigma$  standard deviation of  
343 0.034). The only modern sediment with a ( $^{230}\text{Th}/^{234}\text{U}$ )  $> 1$  is from the uppermost headwater  
344 location and thus is expected to have undergone the least in-channel transport. Colluvial  
345 samples also show ( $^{230}\text{Th}/^{234}\text{U}$ ) ratios  $> 1$ . The ( $^{234}\text{U}/^{238}\text{U}$ ) and ( $^{230}\text{Th}/^{234}\text{U}$ )  $> 1$  in colluvial  
346 deposits could imply a net removal of U due to leaching over gain, and a more fractionated  
347 ( $^{234}\text{U}/^{238}\text{U}$ ) ratio ( $> 1$ ) in the gained component than in the leached (Dequincey et al., 2002).  
348 This could further imply that, for the sediments in the Murrumbidgee catchment, ( $^{230}\text{Th}/^{234}\text{U}$ )  
349 ratios are  $> 1$  before sediments enter the river channel, where significant exchange of U  
350 between sediment and water would result in a net gain of  $^{234}\text{U}$ , producing ( $^{230}\text{Th}/^{234}\text{U}$ ) ratio  $<$   
351 1. For alluvial deposits, ( $^{230}\text{Th}/^{234}\text{U}$ ) ratios decrease with increasing ( $^{234}\text{U}/^{238}\text{U}$ ) ( $R = -0.9$ ),  
352 indicating the evolution of these ratios with time (Fig. 3).

353

### 354 *5.3. Weathering age of Sediments in the Murrumbidgee River catchment*

355 The variation of U-series isotopic composition of sediments is a function of time and  
356 any loss or gain of isotopes. Vigier et al. (2001), Dosseto et al. (2006a, b) and Granet et al.  
357 (2007, 2010) used a model to quantify the time-variation of U-series isotopes in sediment and  
358 soil samples, considering the loss of isotopes by chemical weathering. Their model  
359 considered the present concentration of any radioactive isotope as a function of its production  
360 by decay from the parent (if present), and loss through its own radioactive decay and  
361 leaching. Dequincey et al. (2002) and Dosseto et al. (2008a; b) modified these models by  
362 incorporating any possible gain of isotope to the sediments by processes such as precipitation

363 of secondary phases, dust deposition or physical illuviation in soil profiles. In this model, the  
364 time variation of the abundance of a given isotope  $N_j$  is:

$$365 \quad \frac{dN_j}{dt} = \lambda_i \cdot N_i - \lambda_j \cdot N_j - w_j \cdot N_j + \Gamma_j \cdot N_{j,0} \quad (1)$$

366 where subscripts  $i$  and  $j$  refer to the parent and daughter isotopes, respectively,  $\lambda$  is the decay  
367 constant ( $\text{yr}^{-1}$ ),  $N_{j,0}$  is the initial isotope abundance in the unweathered bedrock,  $\Gamma$  and  $w$  are  
368 gain and loss coefficients, respectively (in  $\text{yr}^{-1}$ ). The gain coefficient,  $\Gamma$ , represents the rate at  
369 which an isotope is incorporated to the sediments via dust deposition and/or secondary phase  
370 coating. Hence, the terms  $\Gamma_j \cdot N_{j,0}$  in the combined form represents the rate at which the  
371 abundance of the isotope is increased due to gain. The loss or dissolution coefficient  $w$   
372 determines the rate at which isotope loss occurs during chemical weathering. The coefficients  
373  $w$  and  $\Gamma$  are assumed to be constant over the duration of weathering for each nuclide  
374 (Chamberlain et al., 2005; Ferrier and Kirchner, 2008). White and Brantley (2003) also  
375 suggested constant  $w$  values for a given mineral based on laboratory experiments of mineral  
376 weathering. The term  $t$  represents the time elapsed since the onset of weathering by which  
377 isotope fractionation occurred, and is termed the *sediment weathering age*,  $T_w$  (Table 1).  
378 Detailed discussion on the model is given in Dosseto et al. (2008b). This model can be solved  
379 for sediment samples from a given catchment area to determine the set of  $w$  and  $\Gamma$  values for  
380 each nuclide and the weathering age ( $T_w$ ) for each sample by reproducing the observed  
381 ( $^{230}\text{Th}/^{234}\text{U}$ ) and ( $^{234}\text{U}/^{238}\text{U}$ ) activity ratios. For the set of 10 samples from the modern  
382 sediments, there are 20 input parameters ( $^{230}\text{Th}/^{234}\text{U}$ ) and ( $^{234}\text{U}/^{238}\text{U}$ ) and 16 output  
383 parameters (10 weathering ages, three  $w$  values and three  $\Gamma$  values). The  $w$  and  $\Gamma$  for this set  
384 of samples for a given nuclide is assumed to be the same. For solving the model, boundary  
385 conditions are applied to  $w$  and  $\Gamma$  values of each nuclide to include values reported so far for  
386 these parameters either in nature or in laboratory experiments in the range for a set of  
387 samples. The reported values of  $w_{238}$ , and  $w_{234}$  vary between  $10^{-6}$  and  $10^{-4} \text{ yr}^{-1}$  and  $w_{230}$  varies  
388 between  $10^{-18}$  and  $10^{-4}$  (Vigier et al., 2001, 2005, 2006, 2011; Dequincey et al., 2002;  
389 Chabaux et al., 2006; Dosseto et al., 2006a, b, c, 2008a, b, 2012; Ma et al., 2010; Suresh et  
390 al., 2013). For  $\Gamma$  values of  $^{238}\text{U}$  and  $^{234}\text{U}$ , the range used is  $10^{-8}$  to  $10^{-4}$ , and for  $^{230}\text{Th}$ , the  
391 range used is  $10^{-14}$  to  $10^{-4}$  which includes published values for  $^{238}\text{U}$ ,  $^{234}\text{U}$  and  $^{230}\text{Th}$  isotopes  
392 (Dosseto et al., 2008a, b, 2012; Ma et al., 2010; Suresh et al., 2013).

393 For the Murrumbidgee sediment samples, the model was solved using codes written  
394 in Matlab for alluvial, colluvial and modern samples separately. The composition of the  
395 Devonian granitic bedrock from Cooma in the upper Murrumbidgee catchment, reported by  
396 Chappell (1984) is taken as the initial condition at the onset of bedrock weathering,  
397 representative of the catchment area. Since the bedrock is older than 1 Myr, ( $^{230}\text{Th}/^{234}\text{U}$ ) and  
398 ( $^{234}\text{U}/^{238}\text{U}$ ) ratios are considered to be at secular equilibrium (cf. Handley et al., 2013). The  
399 gain ( $I$ ) and dissolution ( $w$ ) coefficients can take different values for each nuclide. A  
400 constant  $w$  value implies a time-dependant evolution of chemical dissolution rate of an  
401 isotope, with a higher  $w$  value corresponding to the rate of reaction slowing down faster to  
402 reach a steady state, and vice-versa (White and Brantley, 2003).

403 While solving, the model equation (1) iteratively produces ( $^{230}\text{Th}/^{234}\text{U}$ ) and  
404 ( $^{234}\text{U}/^{238}\text{U}$ ) ratios and compares them with the measured ( $^{230}\text{Th}/^{234}\text{U}$ ) and ( $^{234}\text{U}/^{238}\text{U}$ ) to  
405 minimize the difference between the model-produced and measured ratios. Since the equation  
406 is highly non-linear, a set of solutions for each  $T_w$ ,  $w$  and  $I$  value is generated. The mean  
407 value of each set will be taken as the final solution. The error value associated with each final  
408 solution is calculated using the  $1\sigma$  standard deviation of the produced set of solutions. The  
409 leaching and gain coefficients for all nuclides and the  $T_w$  values of each sample are given in  
410 Table 4.

411 The weathering age of colluvial deposits from Bredbo Gully encompasses the vertical  
412 soil profile residence time, lateral transport time through the hillslope, and the storage time in  
413 the colluvial deposit. Two Bredbo Gully samples collected at 0.4 m and 1.7 m depth display  
414 weathering ages of  $48 \pm 11$  and  $57 \pm 13$  kyr, respectively (Table 4; Fig. 9). The modern  
415 sediment from the upper Bredbo River (Frogs Hollow) has a weathering age of  $77 \pm 31$  kyr.  
416 There are no alluvial deposits observed upstream of this sampling site and sediments are thus  
417 expected to be delivered to the channel directly from the hillslope. All the other modern  
418 sediments and alluvial deposits have weathering ages that vary from  $313 \pm 142$  to  $451 \pm 191$   
419 kyr. Note that ages of  $316 \pm 52$  and  $480 \pm 78$  kyr for modern sediments from the  
420 Murrumbidgee River were determined by Dosseto et al. (2010), using the comminution  
421 dating approach developed by DePaolo et al. (2006), which agree with our results.

422 Anthropogenic activities such as land clearing and agricultural practices have directly  
423 or indirectly led to increased soil erosion rates and catchment sediment yield, compared with



424 pre-European settlement rates (Wasson et al., 1998; Olley et al., 2003). Conversely, the  
425 Burrinjuck Dam (constructed in 1920) is considered to be an excellent trap of river sediments  
426 (e.g. Wasson et al., 1987; Srikanthan and Wasson, 1993; Olley et al., 1997; 2003) and  
427 thousands of small farm dams have been constructed throughout the catchment. However,  
428 these significant changes to sediment load have not affected the overall source types or U-  
429 series characteristics of sediments in the river. Our results show that the sediments upstream  
430 and downstream of the Dam have the same weathering age, indicating that the trapping of  
431 sediments by the construction of the dam has not affected the nature of sediments  
432 downstream. Dosseto et al. (2010) also reported residence times of > 300 kyr for both pre-  
433 European (deposition age ~2.5 kyr) and post-European settlement sediments from the  
434 Murrumbidgee River downstream of the Burrinjuck dam.

435         The leaching coefficients ( $w$ ) for  $^{238}\text{U}$  and  $^{234}\text{U}$  estimated from the model for the  
436 sediments are consistent (within the large model errors; Table 4), showing that removal of  
437 these isotopes from the sediments takes place at comparable rates over the timescales of  
438 sediment evolution. The gain coefficients ( $I$ ) for these isotopes in the sediment samples are  
439 also the same, within the large errors associated. Leaching coefficients estimated for modern  
440 sediments are similar to those determined for the suspended sediments in the Mackenzie  
441 River (Vigier et al., 2001) and for Amazon highland rivers (Dosseto et al., 2006b). Leaching  
442 coefficients of  $^{238}\text{U}$  for the Ganga River and Narmada and Tapti rivers are an order of  
443 magnitude lower than those determined for the Murrumbidgee sediments. These differences  
444 probably indicate that leaching of U-series isotopes from sediments is controlled by the  
445 conditions of weathering in the rivers. Dosseto et al. (2008a) and Vigier et al. (2011)  
446 compiled  $^{238}\text{U}$  leaching coefficients for sediments of different residence time and found a  
447 linear relationship. The leaching coefficient of  $^{238}\text{U}$  observed here also conforms to the same  
448 relationship. White and Brantley (2003) reported that the dissolution rate of silicate minerals  
449 decreases significantly over kilo year timescales. This could possibly correspond to a  
450 decrease of leaching rate of  $^{238}\text{U}$ . A general explanation is still to be reported for the  
451 observation of decreasing leaching coefficient with increasing weathering age. Keech et al.  
452 (2013) reported the leaching coefficients of U-series isotopes from soil samples in the soil  
453 chronosequence in Merced and proposed that the leaching process may not be uniform over  
454 the timescales of weathering. They argued that weathering rate can vary over time and hence  
455 assuming a first order leaching coefficient may not be appropriate in the case of sediments.

456 However, since the weathering rate represents the rate of mass loss and leaching coefficient  
457 represents the timescales of loss of an isotope, a first order assumption is still plausible. The  
458 coefficients reported here for the modern sediments, alluvial deposits and colluvial samples  
459 having different residence times are similar, and could possibly indicate steady state isotope  
460 leaching and gain coefficients over the time of weathering.

461

#### 462 *5.4. Timescales of sediment transfer and storage in the catchment*

463 The stages of sediment evolution can be recognised as: (1) the soil profile residence  
464 time, (2) the lateral (colluvial) transport time, (3) transport time through the river and  
465 intermediate depositions and (4) time since the final deposition (Table 1). Suresh et al.  
466 (2013), using U-series isotopes, determined soil residence times of ~30 kyr on ridge tops in  
467 the upper catchment area of the Murrumbidgee River. Based on cosmogenic nuclide  
468 estimates of soil production rates (Heimsath et al), Yoo et al. (2007) modelled lateral  
469 residence time (Table 1) of soil at the same locality, using soil and saprolite geochemistry, to  
470 derive a lateral transport time of 60 kyr for a soil column of 1 m<sup>2</sup> base area to be transported  
471 50 m downslope. The turnover times of sediments during river transport and alluvial deposits  
472 are discussed below.

473 The results presented here suggest that there is relatively rapid transfer of sediment  
474 through the channel system from the upper catchment to the lower catchment, including time  
475 spent in alluvial storage, with no detectable aging of sediments down the river (although  
476 weathering ages do carry very large uncertainties). Alluvial deposits occur along the upper  
477 Murrumbidgee (Fig. 10) and were sampled but showed weathering ages in the same range as  
478 the modern river sediments and with no downstream age trend, suggesting that alluvial  
479 storage in the upper catchment is of short duration. This can be tested by calculating the time  
480 required to fill the alluvial pockets in the upper catchment area. The total area of the sub-  
481 catchment contributing sediments to the Murrumbidgee River upstream of Burrinjuck Dam is  
482 9673 km<sup>2</sup> (Verstraetan et al., 2007). Using the range of catchment denudation rates of 9 to 24  
483 mm kyr<sup>-1</sup> (Fujioka et al., 2012) and the area available for erosion, the volume of sediments  
484 exported by the river from the upper catchment area per year can be estimated to be 8.7 x 10<sup>-5</sup>  
485 to 2.3 x 10<sup>-4</sup> km<sup>3</sup>yr<sup>-1</sup>. The width of alluvial deposits in the upper catchment area has been  
486 estimated using Google Earth (Fig. 10). The total volume of sediment stored in these alluvial

487 pockets can be calculated by taking the average width (500 m), thickness (considered to be 4  
488 m, from the observed thicknesses of the two alluvial deposits sampled and the depth of the  
489 channel) and total length of the alluvial pockets (50 km, estimated from Google Earth),  
490 yielding a value of  $0.1 \text{ km}^3$ . Thus it can be inferred that the time required to fill the alluvial  
491 pockets is  $< 1 \text{ kyr}$  (assuming 100% sediment trap efficiency), which implies that reworking  
492 of these alluvial sediments cannot account for the weathering ages over 300-500 kyr observed  
493 in modern river sediments. AMS radiocarbon measurements show that the upper limit of  
494 deposition age of floodplain deposits at Wangrah Creek is  $12.4 \pm 0.15 \text{ kyr}$  (Prosser et al.,  
495 1994), with several substantial sediment flushing and filling episodes in the Holocene. They  
496 also reported the existence of remnant slope deposits older than 30 kyr in the Wangrah Creek  
497 catchment. This further implies that reworking of old alluvial deposits cannot account for  
498 residence timescales over 300-500 kyr for modern sediments.

499         Since the time spent by the sediments in the weathering profile, alluvial deposits and  
500 in transport by the river cannot account for the long residence time of sediments; it can be  
501 inferred that the ageing of sediment is occurring during hillslope transport. As mentioned  
502 above, Yoo et al. (2007) reported that colluvial transport time is 60 kyr through a 50 m  
503 downhill transect. The weathering ages of the two colluvial samples in this study are  $48 \pm 11$   
504 and  $57 \pm 13 \text{ kyr}$  and the weathering age for sediment in the Bredbo River adjacent to the study  
505 locality of Yoo et al. (2007) at Frog's Hollow is 77 kyr, supporting this general timeframe.

506         To test whether hillslope transport could account for sediment weathering ages of  
507 hundreds of thousands of years, we determined the distribution of slope lengths in the  
508 Murrumbidgee catchment. Using 1s DEM data and ArcGIS the calculated median slope  
509 length in the upper Murrumbidgee catchment was estimated to be  $265 \pm 128 \text{ m}$ . Assuming a  
510 linear relationship between slope length and sediment transport time and Yoo et al.'s (2007)  
511 rates, it can be estimated that the sediments spend  $\sim 220 \pm 106 \text{ kyr}$  residing on the hillslope  
512 prior to reaching the river channel. The assumption of a linear relationship between slope  
513 length and sediment transport time is justifiable as the universal soil loss equation model  
514 (USLE) considers that hillslope sediment delivery is linearly related to the slope length and  
515 steepness (Gallant, 2001; Lu et al., 2006; Verstraeten et al., 2007). On the basis of the  
516 calculated transport time, it can be concluded that the lateral residence time driven by  
517 transport through hillslope most likely accounts for the long residence time of modern  
518 sediments in the Murrumbidgee River, whereas the vertical soil residence time driven by soil

519 production from the saprolite and fluvial transport time by the river account for a smaller  
520 proportion.

521 A shorter comminution age ( $42 \pm 7$  kyr) for a post-LGM palaeochannels of the lower  
522 Murrumbidgee River has been reported by Dosseto et al. (2010) in contrast to residence times  
523 over 300 kyr for modern sediments and over 100 kyr for pre-LGM palaeochannels sediments.  
524 They proposed that reworking of old (high residence time) alluvial deposits in the middle and  
525 lower valley was the dominant sediment source pre- and post-LGM, and younger (low  
526 residence time) hillslope soil or sediment from the upper catchment was the sediment source  
527 during the LGM. Faster downslope transport of sediments from the catchment area during the  
528 LGM is plausible, as the vegetation cover during LGM in the area was herb and grass-  
529 dominated (Singh and Geissler, 1985) and hence could have promoted erosion (Dosseto et al.,  
530 2010 and references therein). Nevertheless, the residence time of more than 300 kyr for the  
531 post LGM sediment deposits at Wangrah Creek suggests that such an effect must have been  
532 quite limited. Furthermore, extensive erosion of the hillslopes would remove very old soil  
533 material and therefore remove the source of very old sediment deposited in the upper  
534 catchment alluvium during the Holocene and transported today. Our results constrain the  
535 sources of young LGM sediment to fresh bedrock erosion (e.g. channel bed) or ridgetop soils,  
536 rather than colluvial soils or alluvium within the upper catchment.

537

### 538 *5.5. Assessing the potential contribution of aeolian material*

539 Holocene dust deposits from the Snowy Mountains in the upper catchment of the  
540 Murrumbidgee River have been analysed by Marx et al. (2011). Using the trace element data  
541 of the dust samples, they showed that the source of dust is the Murray-Darling basin and that  
542 all the dust samples have U/Th ratios  $> 1$ . The late Pleistocene dust sample analysed here has  
543 a U/Th ratio  $< 1$ , which may point towards a different source of dust prior to the Holocene.  
544 The sample preparation procedure followed by Marx et al. (2011) did not include removal of  
545 exchangeable phases, which may have an effect on U/Th ratios. The possibility of aeolian  
546 dust contribution to the Murrumbidgee sediments was tested following the binary mixing  
547 models suggested by Albarede (1995) for concentrations and ratios. No relationships were  
548 deducible from the model using U-series concentrations or activity ratios of the sediments  
549 and the dust, when considering the U and Th data of soil from Frogs Hollow (reported by

550 Suresh et al., 2013) or of the most downstream sediment sample or of the colluvial samples as  
551 the other end member for mixing. Correlations were absent when subsets of U – Th data  
552 (tributary-trunk stream, colluvial, alluvial or modern sediments) were considered in the  
553 binary mixing model. The non-uniform spread in the U and Th concentrations of the  
554 sediments with some of the values less than that of the dust (as shown in Fig. 8) also indicate  
555 that no significant mixing of sediments with dust is occurring, but more samples are required  
556 to thoroughly understand the potential dust contribution.

557

### 558 *5.6. Broader Implications*

559 A consolidated study of the evolution timescales of all the compartments of sediments  
560 in a single catchment (colluvial, alluvial and modern channel sediments) is reported for the  
561 first time here. The results have local as well as global implications. The residence  
562 timescales of the Murrumbidgee sediments discussed here modify the current understanding  
563 of influence of LGM on sediment transport by rivers in temperate Australia. Dosseto et al.  
564 (2010) concluded that during the LGM, fresh sediments were loaded to the Murrumbidgee  
565 River due to high hillslope connectivity. Their argument of reworking of alluvial deposits  
566 being the source of modern sediments of very long residence time after the LGM envisages  
567 large alluvial deposits in the upper catchment area, which are absent. The long residence  
568 times of alluvial and colluvial deposits in the upper catchment area reported here necessitate  
569 alternate explanations for the arguments of Dosseto et al. (2010). The young residence times  
570 of post-LGM sediments from the palaeochannels of the Murrumbidgee River could only be  
571 explained by proposing that they are either produced by bedrock incision or sourced from the  
572 ridgetops containing young soil. Prosser et al. (1994) suggested that the hillslopes were not  
573 well connected with the river channel during the LGM. This suggestion supports inferred  
574 long residence times of sediments, as this will correspond to aging of sediments in the  
575 hillslopes.

576 Long residence times of river sediments may correspond to slow erosion in the  
577 catchment (Dosseto et al., 2008a). Tectonic and climate regimes are known to affect  
578 denudation rates (von Blackenburg, 2006; Portenga and Bierman, 2011). The globally  
579 averaged erosion rate on catchments in tectonically active areas is over an order of magnitude  
580 higher than that for catchments in tectonically inactive areas (Portenga and Bierman, 2011).

581 Sediment residence times of 1-8 kyr have been reported for tectonically active catchments in  
582 Iceland (Vigier et al., 2006). Granet et al. (2007) reported ~ 1 kyr transfer time of sediments  
583 by the river Ganga draining the tectonically active upper Himalayan region. The long  
584 residence times (~320 kyr) of sediments in the Murrumbidgee River reported here may  
585 reflect the stable tectonic conditions of the catchment. Topography plays a major role in  
586 weathering and erosion. A global compilation of the slope and the relief data of drainage  
587 basins showed positive correlation with erosion rates (Portenga and Bierman, 2011). The  
588 relationship observed between the estimated slopelength and the large lateral residence time  
589 in the Murrumbidgee catchment supports their suggestion (provided the large lateral  
590 residence times of sediments correspond to a slow erosion rate).

## 591 **6. Conclusions**

- 592 1. The mineralogical, elemental and U-series isotopic characteristics of  
593 sediments carried by the Murrumbidgee River in the south-eastern Australia  
594 were determined. The mineralogy of the sediments is consistent with the  
595 granitic lithology of the catchment.
- 596 2. The Si-based Weathering Index does not vary systematically downstream,  
597 suggesting insignificant chemical weathering of sediments during transport in  
598 the Murrumbidgee River.
- 599 3. The concentrations and activity ratios of U-series isotopes of the river  
600 sediments do not show evidence of downstream evolution. Rapid exchange of  
601 U-series isotopes between water and sediments to reach a chemical  
602 equilibrium may be occurring. Alternatively, the lack of systematic  
603 downstream trends in geochemistry could imply rapid sediment transport by  
604 the river system.
- 605 4. Muscovite content in the sediments shows a positive correlation with U  
606 concentration. Muscovite content plays a major role in controlling U-series  
607 isotopes in sediments. A similar observation was reported for soils in the  
608 upper catchment of the Murrumbidgee River (Suresh et al., 2013).
- 609 5. Long lateral residence time of colluvial soil is inferred (~220 kyr). Soil  
610 residence time driven by hillslope transport and average slope length of the  
611 catchment indicates that of the total residence time in the catchment,  
612 sediments spend ~220 kyr in hillslope transport. This could further imply

613 slow erosion, consistent with the average erosion rate of 9 – 24 mm/kyr  
614 estimated using cosmogenic radionuclides (Fujioka et al., 2012).

615 6. The observation of long residence times (~400 kyr) of post-LGM deposits at  
616 Wangrah Creek in the Murrumbidgee catchment contrasts with the young  
617 residence times of post-LGM palaeochannel deposits reported by Dosseto et  
618 al. (2010). The proposal of Dosseto et al. (2010) that erosion of young soil  
619 from ridge top as the source of LGM sediments need to be revised. The  
620 sources of young sediments during LGM in the catchment could be bedrock  
621 incision or fresh bedrock weathering on the ridges.

622 7. Long weathering ages (> 320 kyr) are observed for the alluvial deposits and  
623 modern sediments in the catchment, except for the modern sediment sample  
624 collected from the Bredbo River at Frogs Hollow (77 kyr). The colluvial  
625 deposit samples also have an order of magnitude younger weathering ages  
626 (~50 kyr). Longer residence times of sediments in the catchment could  
627 correspond to the stable landscape, which has been relatively unaffected by  
628 tectonic activity or climatic changes.

629

630

631 Acknowledgements:

632

633 We are grateful to Norman Pearson, Peter Wieland and Russell Field for assistance during  
634 sample preparation and analysis. POS acknowledges an iMQRES scholarship supporting this  
635 research. AD acknowledges an ARC Future Fellowship FT0990447. HH acknowledges an  
636 ARC Linkage grant LP0990500 and an ARC Future Fellowship FT120100400. The  
637 analytical data were obtained using instrumentation funded by DEST Systematic  
638 Infrastructure Grants, ARC LIEF, NCRIS, industry partners and Macquarie University.

639

640

641

642

643

- 645 Albarede, F., 1995. Introduction to geochemical modeling. Cambridge University Press.
- 646 Anderson, M. B., Erel, Y., and Bourdon, B., 2009. Experimental evidence for  $^{234}\text{U}$ - $^{238}\text{U}$   
647 fractionation during granite weathering with implication for  $^{234}\text{U}/^{238}\text{U}$  in natural waters.  
648 *Geochimica et Cosmochimica Acta* 73, 4124-4141.
- 649 Anderson, M. B., Stirling, C. H., Porcelli, D., Halliday, A. H., Andersson, P. S., and  
650 Bhaskaran, M., 2007. The tracing of riverine U in Arctic swawater with very precise  
651  $^{234}\text{U}/^{238}\text{U}$  measurements. *Earth and Planetary Science Letters* 259, 171-185.
- 652 Baeza, A., Del Rio, M., Jimenez, A., Miro, C. and Paniagua, J., 1995. Influence of geology  
653 and soil particle size on the surface-area/volume activity ratio for natural radionuclides.  
654 *Journal of Radioanalytical and Nuclear Chemistry* 189(2), 289-299.
- 655 Bourdon, B., Turner, S., Henderson, G. M., and Lundstrom, C. C., 2003. Introduction to U-  
656 series geochemistry. in B. Bourdon, G.M. Henderson, C.C. Lundstrom, S.P Turner,  
657 (Eds), *Uranium-series Geochemistry, Reviews in Mineralogy and Geochemistry* 52,  
658 Geochemical Society - Mineralogical Society of America, Washington.
- 659 Campbell, J.R., Hesse P.P., and Olley J.M., 2005. Single grain dating of a quaternary loess  
660 profile. 11th International Conference on Luminescence and ESR Dating, Cologne,  
661 Germany.
- 662 Chabaux, F., Granet, M., Pelt, E., France-Lanord, C., and Galy, Valier, 2006.  $^{238}\text{U}$  –  $^{234}\text{U}$  –  
663  $^{230}\text{Th}$  disequilibria and timescale of sediment transfers in rivers: Clues from the  
664 Gangetic plain rivers. *Journal of Geochemical Exploration* 88, 373-375.
- 665 Chabaux, F., Riotte, J. and Dequincey, O., 2003. U-Th-Ra fractionation during weathering  
666 and river transport, in B. Bourdon, G.M. Henderson, C.C. Lundstrom, S.P Turner,  
667 (Eds), *Uranium-series Geochemistry, Reviews in Mineralogy and Geochemistry* 52,  
668 Geochemical Society - Mineralogical Society of America, Washington.
- 669 Chamberlain, C. P., Waldabauer, J. R., and Jacobson, A. D., 2005. Strontium, hydrothermal  
670 systems and steady-state chemical weathering in active mountain belts. *Earth and*  
671 *Planetary Science Letters* 238, 242-248.
- 672 Chappell, B. W., 1984. Source rock of I- and S-type granites in the Lachlan Fold Belt,  
673 southeastern Australia. *Philosophical Transactions of Royal Society of London A* 310,  
674 693-707.
- 675 Cheng, H., Edwards, R. L., Hoff, J., Gallup, C. D., Richards, D. A., and Asmerom, Y., 2000.  
676 The half-lives of uranium -234 and thorium-230. *Chemical Geology* 169, 17-33.



- 677 Dalai, T. K., Rengarajan, R., and Patel, P. P., 2004. Sediment geochemistry of the Yamuna  
678 River System in the Himalaya: Implications to weathering and transport. *Geochemical*  
679 *Journal* 38, 441-453.
- 680 DePaolo, D.J., Maher, K., Christensen, J.N., and McManus, J., 2006. Sediment transport time  
681 measured with U-series isotopes: Results from ODP North Atlantic drift site 984: *Earth*  
682 *and Planetary Science Letters* 248, 394-410.
- 683 Dequincey, O., Chabaux, F., Clauer, N., Sigmarsson, O., Liewig, N. and Leprun, J. C., 2002.  
684 Chemical mobilizations in laterites: Evidence from trace elements and  $^{238}\text{U}$ - $^{234}\text{U}$ -  
685  $^{230}\text{Th}$  disequilibria. *Geochimica et Cosmochimica Acta* 66, 1197-1210.
- 686 Dosseto, A., Buss, H., and Suresh, P.O., 2012. Rapid regolith formation over volcanic  
687 bedrock and implications of landscape evolution. *Earth and Planetary Science Letters*  
688 337-338, 47-55.
- 689 Dosseto, A., Hesse, P., Maher, K., Fryirs, K. and Turner, S. P., 2010. Climatic and  
690 vegetation control on sediment dynamics during last glacial cycle. *Geology* 38, 395-  
691 398.
- 692 Dosseto, A., Bourdon, B. and Turner, S. P., 2008a. Uranium-series isotopes in river  
693 materials: Insights into the timescales of erosion and sediment transport. *Earth and*  
694 *Planetary Science Letters* 265, 1-17.
- 695 Dosseto, A., Turner, S. P. and Chappell, J., 2008b. The evolution of weathering profiles  
696 through time: New insights from uranium-series isotopes. *Earth and Planetary*  
697 *Science Letters* 274, 359-371.
- 698 Dosseto, A., Bourdon, B., Gaillardet, J., Allegre, C. J., and Filizola, N., 2006a. Timescales and  
699 conditions of chemical weathering under tropical climate: study of the Amazon basin  
700 with U-series. *Geochimica et Cosmochimica acta* 70(1), 71-89.
- 701 Dosseto, A., Bourdon, B., Gaillardet, J., Maurice-Bourgoin, L., and Allegre, C. J., 2006b.  
702 Weathering and transport of sediments in the Bolivian Andes: time constraints from  
703 uranium-series isotopes. *Earth and Planetary Science Letters* 248 (3-4), 71-89.
- 704 Dosseto, A., Turner, S. P., and Douglas, G. B., 2006c. Uranium – series isotopes in colloids  
705 and suspended sediments: Timescales for sediment production and transport in the  
706 Murray – Darling River system. *Earth and Planetary Science Letters* 246, 418-431.
- 707 Driscoll, C. T., van Breemen, N., and Mulder, J. 1985. Aluminum chemistry in a forested  
708 spodosol. *Soil Science Society America Journal* 49, 437-444.
- 709 Ferrier, K. L., and Kirchner, J. W., 2008. Effects of physical erosion on chemical denudation  
710 rates: A numerical modeling study of soil-mantled hillslopes. *Earth and Planetary*  
711 *Science Letters* 272, 591-559.

- 712 Fitzsimmons, K.E., Cohen, T.J., Hesse, P.P., Jansen, J., Nanson, G.C., May, J.H., Barrows,  
713 T.T., Haberlah, D., Hilgers, A., Kelly, T., Larsen, J.R., Lomax, J., Treble, P., 2013.  
714 Late Quaternary paleoenvironmental change in the Australian drylands: a synthesis.  
715 Quaternary Science Reviews 74, 78-96.
- 716 Fujioka, T., Dosseto, A., Hesse, P., and Mifsud, C., 2012. Catchment wide denudation rates  
717 from the Murrumbidgee River, Murray Darling Basin, SE Australia, using insitu  
718 cosmogenic  $^{10}\text{Be}$ . Mineralogical Magazine 76, 1725.
- 719 Gallant, J., 2001. Topographic scaling for the NLWRA sediment project. Technical Report  
720 27/01, CSIRO Land and Water, Canberra.
- 721 Gleyzes, C., Tellier, S., and Astruc, M., 2002. Fractionation studies of trace elements in  
722 contaminated soils and sediments: a review of sequential extraction procedures:  
723 Trends in Analytical Chemistry 21, 451-467.
- 724 Granet, M., Chabaux, F., Stille, P., Dosseto, A., France-Lanord, C., and Blaes, E., 2010. U-  
725 series disequilibria in suspended river sediments and implications for sediment  
726 transfer time in the alluvial plains: The case of Himalayan rivers. Geochimica et  
727 Cosmochimica Acta 74, 2851-2865.
- 728 Granet, M., Chabaux, F., Stille, P., France-Lanord, C., and Pelt, E., 2007. Time-scales of  
729 sedimentary transfer and weathering from U-series nuclides: Clues from Himalayan  
730 Rivers: Earth and Planetary Science Letters 261, 389-406.
- 731 Handley, H.K., Turner, S.P., Dosseto, A., Haberlah, D., Afonso, J.C., 2013. Considerations  
732 for U-series dating of sediments: insights from the Flinders Ranges, South Australia.  
733 Chemical Geology 340, 40-48.
- 734 Harnois, L., 1988. The CIW index: a new chemical index of weathering. Sedimentary  
735 Geology v. 55, p. 319-322.
- 736 Heimsath, A. M., Chappell, J., Dietrich, W. E., Nishiizumi, K. and Finkel, R. C., 2000. Soil  
737 production on a retreating escarpment in southeastern Australia. Geology 28(9), 787-  
738 790.
- 739 Hesse, P.P., Humphreys, G.S., Smith, B.L., Campbell, J., Peterson, E.K., 2003. Age of loess  
740 deposits in the Central Highlands of New South Wales. Australian Journal of Soil  
741 Research 41, 1115-1131.
- 742 Hesse, P. P., and McTainsh, G. H., 2003. Australian dust deposits: modern processes and  
743 Quaternary records. Quaternary Science Reviews 22, 2007-2035.
- 744 Jaffey, A. H., Flynn, K. F., Glendenin, L. E., Bentely, W. C., and Essling, A. M., 1971.  
745 Precision measurement of half-lives and specific activities of  $^{235}\text{U}$  and  $^{238}\text{U}$ . Physical  
746 Review A 4, 1889-1906.

- 747 Keech, A. R., West, A. J., Pett – Ridge, J. C., and Henderson, G. M., 2013. Evaluating U –  
748 series tools for weathering rate and duration on a soil sequence of known ages. *Earth*  
749 *and Planetary Science Letters* 374, 24-35.
- 750 Kigoshi, K., 1971. Alpha-Recoil Thorium-234: Dissolution into Water and the Uranium-  
751 234/Uranium-238 Disequilibrium in Nature: *Science* 173, 47-48.
- 752 Lee, M.H., Yoon, Y.Y., Clark, S.B., and Glover, S.E., 2004. Distribution and geochemical  
753 association of actinides in a contaminated soil as a function of grain size.  
754 *Radiochimica Acta* 92, p. 671-675.
- 755 Lu, H., Moran, C. J., and Prosser, I. P., 2006. Modelling sediment delivery ratio over the  
756 Murray Darling Basin. *Environmental Modelling and Software* 21, 1297-1308.
- 757 Ma, L., Chabaux, F., Pelt, E., Blaes, E., Jin, L., and Brantley, S., 2010. Regolith production  
758 rates calculated with uranium-series isotopes at Susquehanna/Shale Hills Critical  
759 Zone Observatory. *Earth and Planetary Science Letters* 297, 211-225.
- 760 Marx, S. K., Kamber, B. S., McGowan, H. A., and Denholm, J., 2011. Holocene dust  
761 deposition rates in Australia’s Murray-Darling Basin record interplay between aridity  
762 and the position of the mid-latitude westerlies. *Quaternary Science Reviews* 30, 3290-  
763 3305.
- 764 Mathieu, D., Bernat, M., and Nahon, D., 1995. Short-lived U and Th isotope distribution in a  
765 tropical laterite derived from granite (Pitinga river basin, Amazonia, Brazil):  
766 Application to assessment of weathering rate. *Earth and Planetary Science Letters*  
767 136, 703-714.
- 768 McLennan, S. C., Sediments and soils: Chemistry and abundances. *in* Rock physics and  
769 phase relations, a handbook of physical constants, AGU reference shelf 3, American  
770 Geophysical Union, 8-19.
- 771 Milton, G. M., and Brown, R. M., 1987. Adsorption of uranium from groundwater by  
772 common fracture secondary minerals. *Canadian Journal of Earth Science* 24, 1321-  
773 1328.
- 774 Nesbitt, H. W., and Young, G. M., 1982. Early proterozoic climates and plate motions  
775 inferred from major element chemistry of lutites. *Nature* 299, 715-717.
- 776 Norrish, K., and Hutton, J. T., 1969. An accurate spectrographic method for the analysis of a  
777 wide range of geological samples. *Geochimica et Cosmochimica Acta* 33, 431-451.
- 778 Olley, J. M., Roberts, R. G., and Murray, A. S., 1997. A novel method for determining  
779 residence times of river and lake sediments based on disequilibrium in the thorium  
780 decay series. *Water Resources Research* 33, 1319-1326.
- 781

- 782 Olley, J. M., and Wasson, R. J., 2003. Changes in the flux of sediments in the upper  
783 Murrumbidgee catchment, south-eastern Australia, since European settlement.  
784 Hydrological Processes 17, 3307- 3320.  
785
- 786 Plater, A.J., Ivanovich, M., and Douglas, R.E., 1992. Uranium series disequilibrium in river  
787 sediments and waters: the significance of anomalous activity ratios. Applied  
788 Geochemistry 7, 101-110.  
789
- 790 Portenga, E. W., and Bierman, P. R., 2011. Understanding Earth's eroding surface with <sup>10</sup>Be.  
791 GSA Today 21, 4-10.  
792
- 793 Prosser, I. P., Chappell, J., and Gillespie, R., 1994. Holocene valley aggradation and gully  
794 erosion in headwater catchments, south-eastern highlands of Australia. Earth Surface  
795 Processes and Landforms 19, 465-480.  
796
- 797 Robinson, L. F., Belshaw, N. S., and Henderson, G. M., 2004. U and Th concentrations and  
798 isotope ratios in modern carbonates and waters from the Bahamas. Geochimica et  
799 Cosmochimica Acta 68, 1777-1789.  
800
- 801 Rosholt, J. N., 1983. Isotopic composition of uranium and thorium in crystalline rocks.  
802 Journal of Geophysical Research 88, 7315-7330.  
803
- 804 Scott, M. R., 1968. Thorium and Uranium concentrations and isotope ratios in river  
805 sediments. Earth and Planetary Science Letters 4, 245-252.  
806
- 807 Sims, K. W. W., Gill, J. B., Dosseto, A., Hoffmann, D. L., Lundstrom, C. C., Williams, R.  
808 W., Ball, L., Tollstrup, D., Turner, S., Prytulak, J., Glessner, J. J. G., Standish, J. J.,  
809 and Elliott, T., 2008. An Inter-Laboratory Assessment of the Thorium Isotopic  
810 Composition of Synthetic and Rock Reference Materials. Geostandards and  
811 Geoanalytical Research 32(1), 65-91.  
812
- 813 Singh, G., and Geissler, E. A., 1985. Cainozoic History of Vegetation, Fire, Lake Levels and  
814 Climate, at Lake George, New South Wales, Australia. Philosophical Transactions of  
815 Royal Society of London B 311, 379-447.
- 816 Srikanthan, R., and Wasson, R. J., 1993. Influence of recent climate on sedimentation in  
817 Burrinjuck Reservoir. IAHS publication no. 217, 109-118.
- 818 Suresh, P. O., Dosseto, A., Hesse, P. P., and Handley, H. K., 2013. Soil formation rates  
819 determined from uranium-series disequilibria in soil profiles from south-eastern  
820 Australian highlands. Earth and Planetary Science Letters 379, 26-37.
- 821 Suresh, P. O., and C. -A. Huh, C. -A. Evolution of soil on young volcanic bedrocks:  
822 Revisiting geochemical and cosmochemical data from Tatun volcanic area, northern  
823 Taiwan. Submitted to Earth Surface Processes and Landforms.
- 824 Taylor, S. R., and McLennan, S. M., 1985. The continental crust: Its composition and  
825 evolution. Blackwell, Oxford, pp. 312

- 826 Turner, S., Beier, C., Niu, Y., and Cook, C., 2011. U-Th-Ra disequilibria and the extent of  
827 off-axis volcanism across the East Pacific Rise at 9°30'N, 10°30'N, and 11°20'N.  
828 *Geochem. Geophys. Geosyst.* 12, Q0AC12.
- 829 Verstraeten, G., Prosser, I. P., and Fogarty, P., 2007. Predicting the spatial patterns of  
830 hillslope sediment deliver to river channels in the Murrumbidgee catchment,  
831 Australia. *Journal of Hydrology* 334, 440-454. Vigier, N., Bourdon, B., 2011.  
832 Constraining rates of chemical and physical erosion using U-series radionuclides. In:  
833 Baskaran M (ed.) *Handbook of environmental isotope geochemistry*. Springer, Berlin
- 834 Vigier, N., Burton, K. W., Gsalson, S. R., Rogers, N. W., Duhence, S., Thomas, L., Hodge,  
835 E., and Schaefer, B., 2006. The relationship between riverine U-series disequilibria  
836 and erosion rates in the basaltic terrain. *Earth and Planetary Science Letters* 249, 258-  
837 273.
- 838 Vigier, N., Bourden, B., Lewin, E., Dupre, B., Turner, S., Chakrapani, G. J., van Calsteren,  
839 P., and Allegre, C. J., 2005. Mobility of U-series nuclides during basalt weathering:  
840 An example from the Deccan Traps (India). *Chemical Geology* 219, 69-91.
- 841 Vigier, N., Bourden, B., Turner, S. and Allegre, C. J., 2001. Erosion timescales derived from  
842 U-decay series measurements in rivers. *Earth and Planetary Science Letters* 193, 549-  
843 563.
- 844 von Blanckenburg, F., 2006. The control mechanisms of erosion and weathering at basin  
845 scale from cosmogenic nuclides in river sediments. *Earth and Planetary Science*  
846 *Letters* 242, 224-239.
- 847 Yoo, K., Amundson, R., Heimsath, A. M. and Dietrich, W. E., 2007. Intergration of  
848 geochemical mass balance with sediment transport to calculate rates of soil chemical  
849 weathering and transport on hillslopes. *Journal of Geophysical Research* 112, F0  
850 2013.
- 851 Wallbrink, P.J., Murray, A. S., and Olley, J. M., 1998. Determining sources and transit times  
852 of suspended sediments in the Murrumbidgee River, New South Wales, Australia,  
853 using fallowut <sup>137</sup>Cs and <sup>210</sup>Pb. *Water Resources Research* 34, 879-887.
- 854 Wasson, R. J., Clark, R. L., Nanninga P. M., and Waters, J., 1987. <sup>210</sup>Pb as a chronometer and  
855 tracer, Burrinjuck reservoir, Australia. *Earth surface processes and landforms* 12, 399-  
856 414.
- 857 Wasson, R. J., Mazari, R. K., Starr, B., and Clifton, C., 1998, The recent history of erosion  
858 and sedimentation on the Southern Tablelands of southeastern Australia: sediment flux  
859 dominated by channel incision: *Geomorphology*, v. 24, p. 291-308.

860 White, A. F., and Brantley, S. L., 2003. The effect of time on weathering of silicate minerals:  
861 why do weathering rates differ in laboratory and field?. *Chemical Geology* 202, 479-  
862 506.

863 White, A. F., 2008. Quantitative approaches to characterizing natural chemical weathering  
864 rates, in Brantley, S. L., Kubicki, J. D., and White, A. F. (Eds) *Kinetics of rock water*  
865 *interactions*, Springer, New York, pp. 469-543.

866 Williams, R.W., Collerson, K.D., Gill, J.B., and Deniel, C., 1992. High Th/U ratios in  
867 subcontinental lithospheric mantle: mass spectrometric measurement of Th isotopes in  
868 Gausberg lamproites: *Earth and Planetary Science Letters* 111, 257-268.

869

870

871

872

873

874

875

876

877

878

879

880

881

882

883

884

885

886

## Tables

887

Table 1. Definition of timescale terminology used.

| Name                    | Definition   | Determined by  |
|-------------------------|--|--|
| Comminution age         | Time since the production of fine grains (<50 $\mu\text{m}$ ) by bedrock weathering            | $^{238}\text{U}$ - $^{234}\text{U}$ disequilibrium   |
| Weathering age          | Time since the onset of chemical weathering of bedrock to produce regolith.                    | $^{238}\text{U}$ - $^{234}\text{U}$ - $^{230}\text{Th}$ disequilibrium   |
| Soil residence time     | Time since the conversion of saprolite into soil.  | Weathering age of topsoil  |
| Lateral residence time  | Time spent by the soil on the hillslope.   | 1. $^{10}\text{Be}$ -derived soil production function and geochemical mass balance model (Heimsath et al., 2000).<br>2. Foothlope colluvial weathering age |
| Sediment residence time | Time spent by the sediment grains from formation by bedrock weathering until final deposition. | Comminution age or weathering age minus deposition age (if applicable)   |

888

889

890

891

892

893

894

895

896

897

898

899

900

901

902

903

904

905

906

907

908

909

910

911

912

913

914

915  
916

Table 2. Sampling localities and U-series data of leached sediment samples from the Murrumbidgee River and three of its tributaries.

| Sample name                 | Place              | Channel Length (km) <sup>‡</sup> | Sample Depth (m) | Th (ppm) <sub>±</sub> * | U (ppm) <sub>±</sub> * | ( <sup>234</sup> U/ <sup>238</sup> U) <sub>±</sub> <sup>‡</sup> | ( <sup>230</sup> Th/ <sup>234</sup> U) <sub>±</sub> <sup>‡</sup> |
|-----------------------------|--------------------|----------------------------------|------------------|-------------------------|------------------------|---|--|
| <i>Alluvium</i>             |                    |                                  |                  |                         |                        |   |  |
| MU8_low                     | Wangraah Creek     | -40                              | 3.6              | 16.62±0.03              | 3.82±0.03              | 1.21±0.01   | 0.67±0.02  |
| MU8_up                      | Wangraah Creek     | -40                              | 1.4              | 21.70±0.04              | 6.33±0.05              | 1.35±0.02   | 0.62±0.02  |
| MU3                         | Bredbo             | 0                                | 4.1              | 10.69±0.02              | 1.77±0.01              | 1.02±0.01   | 1.07±0.03  |
| MU18                        | Bundarbo           | 240                              | 0.4              | 13.81±0.02              | 2.83±0.02              | 1.12±0.01   | 0.86±0.03  |
| MU19_low                    | Gundagai           | 360                              | 7.7              | 21.78±0.03              | 5.59±0.04              | 1.26±0.02   | 0.64±0.02  |
| MU19_mid                    | Gundagai           | 360                              | 3.6              | 18.46±0.03              | 3.12±0.02              | 1.08±0.01   | 0.82±0.02  |
| MU19_up                     | Gundagai           | 360                              | 0.25             | 12.49±0.02              | 2.36±0.02              | 1.09±0.01   | 0.84±0.03  |
| MU22                        | Darlington Point   | 780                              | 3                | 14.91±0.03              | 2.71±0.02              | 1.05±0.01   | 1.09±0.03  |
| <i>Colluvium</i>            |                    |                                  |                  |                         |                        |   |  |
| MU6_low                     | Bredbo Gully       | -1                               | 1.7              | 16.61±0.03              | 2.61±0.02              | 1.27±0.02   | 1.11±0.03  |
| MU6_up                      | Bredbo Gully       | -1                               | 0.4              | 16.95±0.03              | 2.63±0.02              | 1.06±0.01   | 1.09±0.03  |
| <i>Modern</i>               |                    |                                  |                  |                         |                        |   |  |
| MU11                        | Frogs Hollow       | -40                              | 0                | 13.92±0.02              | 1.89±0.02              | 1.18±0.01   | 1.17±0.04  |
| MU4                         | Bredbo             | -1                               | 0                | 15.13±0.03              | 2.92±0.02              | 1.12±0.01   | 0.73±0.02  |
| MU5                         | Bredbo             | -1                               | 0                | 12.89±0.02              | 2.68±0.02              | 1.25±0.02   | 0.70±0.02  |
| MU1                         | Bredbo             | 0                                | 0                | 13.54±0.02              | 3.12±0.02              | 1.16±0.01   | 0.69±0.02  |
| MU12                        | Taemas Bridge      | 160                              | 0                | 9.65±0.02               | 2.16±0.02              | 1.19±0.01   | 0.74±0.02  |
| MU15                        | Brindabella Valley | 160                              | 0                | 12.50±0.02              | 3.11±0.02              | 1.26±0.02   | 0.64±0.02  |
| MU17                        | Bundarbo           | 240                              | 0                | 17.79±0.03              | 4.42±0.04              | 1.19±0.01   | 0.75±0.02  |
| MU20                        | Gundagai           | 360                              | 0                | 12.52±0.02              | 4.23±0.03              | 1.22±0.01   | 0.49±0.02  |
| MU16                        | Brungle            | 360                              | 0                | 18.17±0.03              | 3.66±0.03              | 1.15±0.01   | 0.73±0.02  |
| MU21                        | Darlington Point   | 780                              | 0                | 10.73±0.02              | 2.19±0.02              | 1.09±0.01   | 0.71±0.02  |
| <i>Dust</i>                 |                    |                                  |                  |                         |                        |   |  |
| MU24                        | Carcoar            |                                  | 1.5              | 11.61±0.02              | 1.70±0.01              | 1±0.01  | 1.24±0.03  |
| <i>Gravimetric standard</i> |                    |                                  |                  |                         |                        |   |  |
| TML-3 (n=2)                 |                    |                                  |                  | 29.62±0.44              | 10.469±0.118           | 0.994±0.003   | 1.004±0.006  |

917

<sup>‡</sup>Negative values indicate upstream Bredbo. \* Concentrations are determined by isotope dilution. <sup>‡</sup>Reported with 2σ external errors

918  
919  
920  
921  
922



923 Table 3. Mineralogy, WIS and granulometric mud fraction data of the sediment samples from the Murrumbidgee River  
 924 catchment.

| Sample name      | Quartz (%) | Albite (%) | Microcline (%) | Muscovite (%) | Illite (%) | WIS (%) <sup>a</sup> | Mud fraction (%) <sup>b</sup> |
|------------------|------------|------------|----------------|---------------|------------|----------------------|-------------------------------|
| <i>Alluvium</i>  |            |            |                |               |            |                      |                               |
| MU8_low          | 71.2       | 6.4        | 0              | 22.4          | 0          | 83.4                 | 37.3                          |
| MU8_up           | 45.9       | 0          | 0              | 54.1          | 0          | 72.3                 | 74.4                          |
| MU3              | 72.7       | 19         | 0              | 8.2           | 0          | 86.5                 | 2.2                           |
| MU18             | 78.4       | 14.3       | 4.1            | 3.2           | 0          | 84.4                 | 37.3                          |
| MU19_low         | 62.8       | 12.9       | 3.9            | 20.5          | 0          | 80.4                 | 78.3                          |
| MU19_mid         | 78.1       | 17.3       | 0              | 4.7           | 0          | 84.3                 | 43.4                          |
| MU19_up          | 67.3       | 19.1       | 10.4           | 3.2           | 0          | 85.4                 | 20.3                          |
| MU22             | 72.8       | 8          | 3.3            | 14.3          | 1.6        | 83.2                 | 37.5                          |
| <i>Colluvium</i> |            |            |                |               |            |                      |                               |
| MU6_low          | 61.1       | 0          | 0              | 39            | 0          | 78.0                 | 32.5                          |
| MU6_up           | 61.9       | 6.6        | 0              | 31.6          | 0          | 83.0                 | 30.4                          |
| <i>Modern</i>    |            |            |                |               |            |                      |                               |
| MU11             | 57.7       | 22.3       | 18.4           | 1.6           | 0          | 84.4                 | 1.9                           |
| MU4              | 71.8       | 11.5       | 0              | 5.4           | 11.3       | 82.8                 | 38.1                          |
| MU5              | 73.8       | 10.6       | 0              | 6.4           | 9.2        | 85.4                 | 46.0                          |
| MU1              | 68.9       | 14.1       | 0              | 16.9          | 0          | 82.8                 | 57.5                          |
| MU12             | 72.7       | 14         | 8.2            | 1.8           | 3.3        | 86.3                 | 25.1                          |
| MU15             | 70.2       | 9.9        | 6.6            | 10.1          | 3.3        | 83.5                 | 40.9                          |
| MU17             | 60.3       | 11.6       | 8.9            | 2             | 14         | 80.0                 | 96.4                          |
| MU20             | 76.1       | 9.1        | 1.5            | 11.8          | 1.5        | 84.4                 | 46.8                          |
| MU16             | 69.6       | 10.9       | 4.9            | 9.8           | 5.2        | 80.0                 | 38.0                          |
| MU21             | 84.6       | 8.1        | 2.1            | 3.2           | 2          | 87.6                 | 30.9                          |
| <i>Dust</i>      |            |            |                |               |            |                      |                               |
| MU24             | 100        |            |                |               |            | 92.4                 |                               |

925 <sup>a</sup> From major element data see Table S1. <sup>b</sup> From particle size distribution measurement

926

927

928

929

930

931

Table 4. Modelled leaching and gain coefficients for U and Th isotopes and weathering ages.

|                    | $W_{238}$                                 | $W_{234}$   | $W_{230}$ | $\Gamma_{238}$ | $\Gamma_{234}$ | $\Gamma_{230}$ |
|--------------------|---|-------------|-----------|----------------|----------------|----------------|
| Alluvium           | 0.742±0.007                               | 0.771±0.023 | 9.42±8.69 | 1.58±0.91      | 1.96±1.94      | 4.02±3.85      |
| Colluvium          | 0.746±0.001                               | 0.752±0.007 | *3.6±0.04 | *1.0±0.01      | *0.7±0.4       | *1.3±0.01      |
| Modern             | 0.732±0.004                               | 0.729±0.004 | 17.7±1.4  | 3.17±1.58      | 3.88±1.93      | 6.72±3.33      |
| <b>Sample name</b> | <b><math>T_w</math> (kyr)<sup>§</sup></b> |             |           |                |                |                |
| <i>Alluvium</i>    |   |             |           |                |                |                |
| MU8_low            | 395±166                                   |             |           |                |                |                |
| MU8_up             | 438±177                                   |             |           |                |                |                |
| MU3                | 313±142                                   |             |           |                |                |                |
| MU18               | 370±163                                   |             |           |                |                |                |
| MU19_low           | 413±171                                   |             |           |                |                |                |
| MU19_mid           | 334±146                                   |             |           |                |                |                |
| MU19_up            | 355±155                                   |             |           |                |                |                |
| MU22               | 339±154                                   |             |           |                |                |                |
| <i>Colluvium</i>   |   |             |           |                |                |                |
| MU6_low            | 57±13                                     |             |           |                |                |                |
| MU6_up             | 48±11                                     |             |           |                |                |                |
| <i>Modern</i>      |   |             |           |                |                |                |
| MU11               | 77±31                                     |             |           |                |                |                |
| MU4                | 369±168                                   |             |           |                |                |                |
| MU5                | 397±180                                   |             |           |                |                |                |
| MU1                | 402±181                                   |             |           |                |                |                |
| MU12               | 403±187                                   |             |           |                |                |                |
| MU15               | 418±189                                   |             |           |                |                |                |
| MU17               | 419±189                                   |             |           |                |                |                |
| MU20               | 451±191                                   |             |           |                |                |                |
| MU16               | 381±173                                   |             |           |                |                |                |
| MU21               | 371±169                                   |             |           |                |                |                |

933 All the coefficients are in  $10^{-5} \text{ yr}^{-1}$ 

934 \*Taken from Suresh et al. (2013), reported for the soil profile from Frogs Hollow.

935 The model errors reported are  $2\sigma$ 

936

937

938

939

940

941

## Figure Captions

- 942 Fig. 1. The Murrumbidgee catchment area map (DEM data from Geoscience Australia). BR: Bredbo River. GR:  
943 Goodradigbee River, TR: Tumut River. MR: Murrumbidgee River. WC: Wangraha Creek. FH: Frogs Hollow.  
944 Locations of all the samples used in this study are shown. The numbers marking sample locations correspond to  
945 their MU numbers in Table 2. Suffix to the sample number refers to the type of the sample (m: modern, a:  
946 alluvial deposit, c: colluvial deposit, d: dust deposit)
- 947 Fig. 2. Downstream variation of quartz and albite in the modern sediments from the Murrumbidgee River.
- 948 Fig. 3. U-series activity ratios of the sediment and dust samples. The error bars represent external analytical  
949 errors.
- 950 Fig. 4. Downstream variation of Si-based Weathering Index for modern, alluvial and colluvial sediments from  
951 the Murrumbidgee catchment.
- 952 Fig. 5. Average major element oxide concentrations of sediments normalized to those of the upper continental  
953 crust concentrations from McLennan (1995) and to those of the Cooma Graodiorite (Chappell 1984). A value <  
954 1 indicates elemental mobilization, and a value > 1 indicates elemental gain.
- 955 Fig. 6. Variation of concentration of U and Th with mud content in the modern, colluvial and alluvial  
956 sediments. External analytical errors are smaller than the symbol size.
- 957 Fig. 7. Variation of concentration of U and Th with muscovite content in the modern sediment samples. External  
958 analytical errors are smaller than the symbol size.
- 959 Fig. 8. Variation of concentration of U and Th with WIS for the river modern, colluvial and alluvial sediments  
960 and dust samples. Soil data from Frogs Hollow in the upper catchment (Suresh et al., 2013) are also shown.  
961 External analytical errors are smaller than the symbol size.
- 962 Fig. 9. Weathering ages ( $T_w$ ) of sediments from the Murrumbidgee River along the length of the stream. The  
963 error associated with  $T_w$  is the  $1\sigma$  standard deviation
- 964 Fig. 10. Width of alluvial deposit pockets in the upper catchment area (upstream of Gundagai) of the  
965 Murrumbidgee River and two of its tributaries.

967 Table S1. Major element data of all the samples from the Murrumbidgee catchment area.

| Sample name      | SiO <sub>2</sub> (wt.%) | TiO <sub>2</sub> (wt.%) | Al <sub>2</sub> O <sub>3</sub> (wt.%) | Fe <sub>2</sub> O <sub>3</sub> (wt.%) | Mn <sub>2</sub> O <sub>4</sub> (wt.%) | MgO (wt.%) | CaO (wt.%) | Na <sub>2</sub> O (wt.%) | K <sub>2</sub> O (wt.%) | P <sub>2</sub> O <sub>5</sub> (wt.%) | Cr <sub>2</sub> O <sub>3</sub> (wt.%) | ZrO <sub>2</sub> (wt.%) | SiO (wt.%) | ZnO (wt.%) | NiO (wt.%) | BaO (wt.%) |
|------------------|-------------------------|-------------------------|---------------------------------------|---------------------------------------|---------------------------------------|------------|------------|--------------------------|-------------------------|--------------------------------------|---------------------------------------|-------------------------|------------|------------|------------|------------|
| <i>Alluvium</i>  |                         |                         |                                       |                                       |                                       |            |            |                          |                         |                                      |                                       |                         |            |            |            |            |
| MU8_low          | 68.7                    | 0.7                     | 12.62                                 | 9.13                                  | 0.05                                  | 1.25       | 0.3        | 0.8                      | 2.67                    | 0.3                                  | 0.01                                  | 0.03                    | 0.01       | 0.01       | 0.01       | 0.03       |
| MU8_up           | 57.42                   | 0.89                    | 20.51                                 | 8.36                                  | 0.09                                  | 1.93       | 0.7        | 0.8                      | 3.5                     | 0.2                                  | 0.02                                  | 0.03                    | 0.02       | 0.02       | 0.01       | 0.06       |
| MU3              | 78.22                   | 0.44                    | 9.94                                  | 2.84                                  | 0.05                                  | 0.8        | 1          | 1.3                      | 2.61                    | 0.1                                  | 0.01                                  | 0.03                    | 0.02       | 0.01       | BLD        | 0.03       |
| MU18             | 75.71                   | 0.7                     | 11.36                                 | 3.15                                  | 0.08                                  | 0.88       | 0.9        | 1.7                      | 2.65                    | 0.1                                  | 0.01                                  | 0.05                    | 0.02       | 0.02       | 0.01       | 0.04       |
| MU19_low         | 69.13                   | 0.87                    | 14.91                                 | 5.14                                  | 0.15                                  | 1.3        | 0.8        | 1.2                      | 2.62                    | 0.2                                  | 0.03                                  | 0.04                    | 0.02       | 0.01       | 0.03       | 0.05       |
| MU19_mid         | 76.4                    | 0.67                    | 11.66                                 | 3.21                                  | 0.07                                  | 0.87       | 0.9        | 1.7                      | 2.81                    | 0.1                                  | 0.01                                  | 0.06                    | 0.02       | 0.01       | 0.01       | 0.04       |
| MU19_up          | 77.99                   | 0.46                    | 10.75                                 | 2.42                                  | 0.05                                  | 0.69       | 0.8        | 1.8                      | 3.16                    | 0.1                                  | 0.01                                  | 0.04                    | 0.01       | 0.01       | BLD        | 0.04       |
| MU22             | 72.52                   | 0.75                    | 13.28                                 | 4.15                                  | 0.02                                  | 0.84       | 0.5        | 0.9                      | 2.33                    | 0                                    | 0.01                                  | 0.05                    | 0.07       | 0.01       | BLD        | 0.04       |
| <i>Colluvium</i> |                         |                         |                                       |                                       |                                       |            |            |                          |                         |                                      |                                       |                         |            |            |            |            |
| MU6_low          | 64.11                   | 0.64                    | 17.42                                 | 6.63                                  | 0.15                                  | 1.21       | 0.4        | 0.3                      | 3.15                    | 0.1                                  | 0.02                                  | 0.03                    | 0.01       | 0.03       | 0.01       | 0.04       |
| MU6_up           | 71.2                    | 0.73                    | 13.5                                  | 5.51                                  | 0.19                                  | 1.45       | 0.4        | 0.7                      | 2.99                    | 0.1                                  | 0.02                                  | 0.03                    | 0.01       | 0.01       | 0.01       | 0.03       |
| <i>Modern</i>    |                         |                         |                                       |                                       |                                       |            |            |                          |                         |                                      |                                       |                         |            |            |            |            |
| MU11             | 76.58                   | 0.18                    | 10.41                                 | 1.73                                  | 0.04                                  | 0.39       | 1.3        | 2.4                      | 3.5                     | 0                                    | BLD*                                  | 0.01                    | 0.01       | BLD        | BLD        | 0.03       |
| MU4              | 71.62                   | 0.86                    | 12.41                                 | 4.8                                   | 0.09                                  | 1.41       | 1.3        | 1.2                      | 2.18                    | 0.1                                  | 0.02                                  | 0.05                    | 0.02       | 0.01       | 0.01       | 0.04       |
| MU5              | 75.82                   | 0.52                    | 10.96                                 | 3.89                                  | 0.32                                  | 0.9        | 0.9        | 1.1                      | 2.58                    | 0.1                                  | 0.01                                  | 0.03                    | 0.01       | 0.01       | 0.01       | 0.03       |
| MU1              | 71.56                   | 0.72                    | 12.81                                 | 4.62                                  | 0.2                                   | 1.3        | 1          | 1.1                      | 2.63                    | 0.1                                  | 0.01                                  | 0.03                    | 0.02       | 0.01       | 0.01       | 0.04       |
| MU12             | 78.43                   | 0.42                    | 10.37                                 | 2.59                                  | 0.06                                  | 0.66       | 0.8        | 1.3                      | 2.71                    | 0.1                                  | BLD                                   | 0.02                    | 0.01       | 0.1        | 0.01       | 0.03       |
| MU15             | 72.32                   | 0.71                    | 11.79                                 | 3.43                                  | 0.12                                  | 0.93       | 1.5        | 1                        | 2.93                    | 0.2                                  | 0.01                                  | 0.04                    | 0.02       | 0.01       | 0.01       | 0.04       |
| MU17             | 68.25                   | 0.95                    | 14.57                                 | 4.47                                  | 0.17                                  | 1.09       | 1.2        | 1.3                      | 3.33                    | 0.2                                  | 0.01                                  | 0.03                    | 0.02       | 0.01       | 0.01       | 0.05       |
| MU20             | 73.98                   | 0.73                    | 11.1                                  | 3.87                                  | 0.16                                  | 1.09       | 1.1        | 1.5                      | 2.34                    | 0.1                                  | 0.03                                  | 0.04                    | 0.02       | 0.01       | 0.01       | 0.03       |
| MU16             | 67.65                   | 0.86                    | 14.27                                 | 5.6                                   | 0.4                                   | 1.6        | 1.5        | 1.2                      | 2.3                     | 0.2                                  | 0.03                                  | 0.06                    | 0.02       | 0.01       | 0.02       | 0.04       |
| MU21             | 79.04                   | 0.53                    | 9.5                                   | 2.4                                   | 0.04                                  | 0.58       | 0.6        | 1.1                      | 2.44                    | 0.1                                  | 0.01                                  | 0.05                    | 0.01       | BLD        | BLD        | 0.02       |
| <i>Dust</i>      |                         |                         |                                       |                                       |                                       |            |            |                          |                         |                                      |                                       |                         |            |            |            |            |
| MU24             | 83.61                   | 1.09                    | 6.37                                  | 3.86                                  | 0.08                                  | 0.2        | 0.1        | 0.3                      | 0.9                     | 0                                    | 0.01                                  | 0.08                    | 0.01       | BLD        | BLD        | 0.01       |

968 \*BLD stands for below the limit of detection

Figure 1  
[Click here to download high resolution image](#)

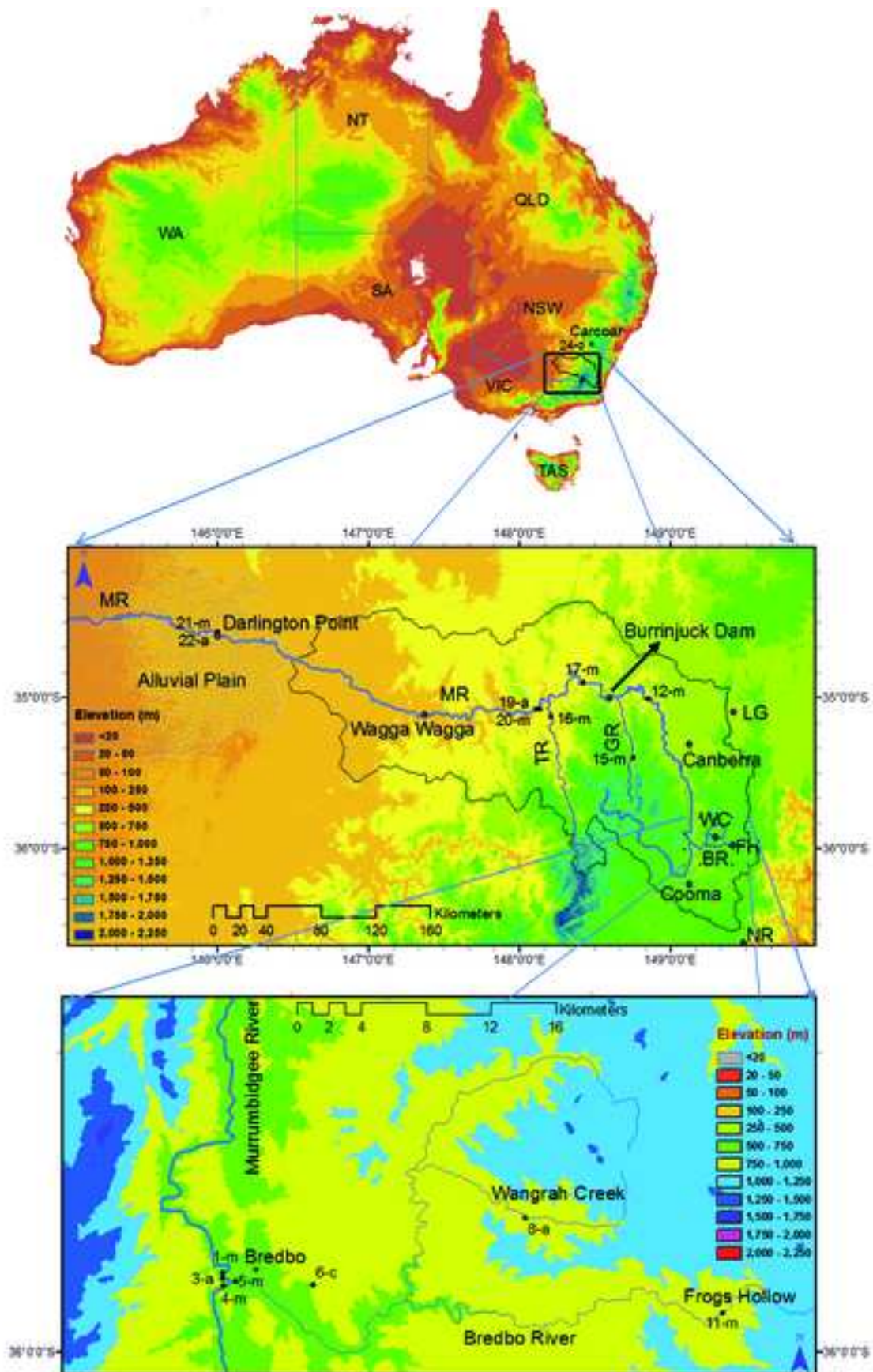


Figure 2  
[Click here to download high resolution image](#)

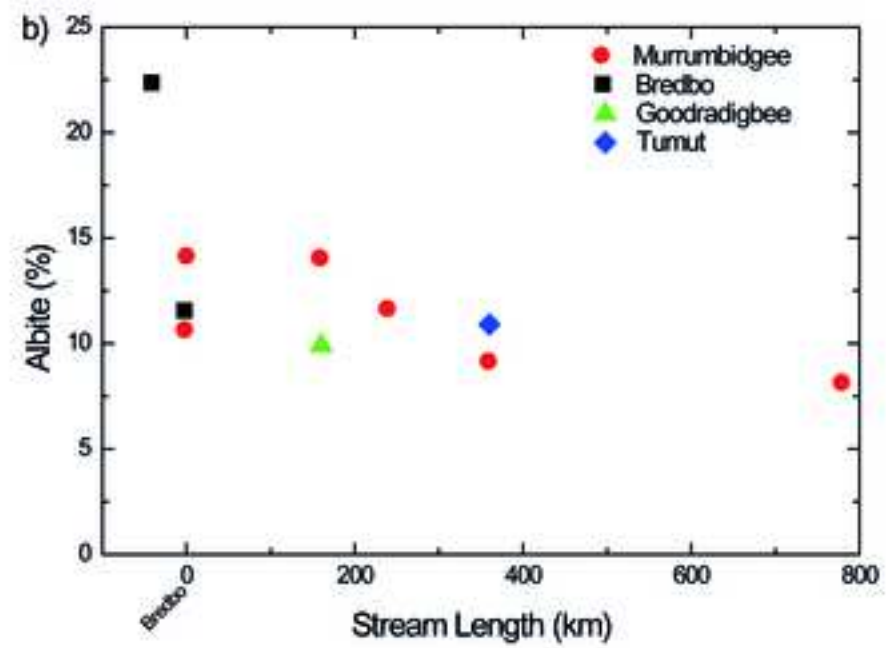
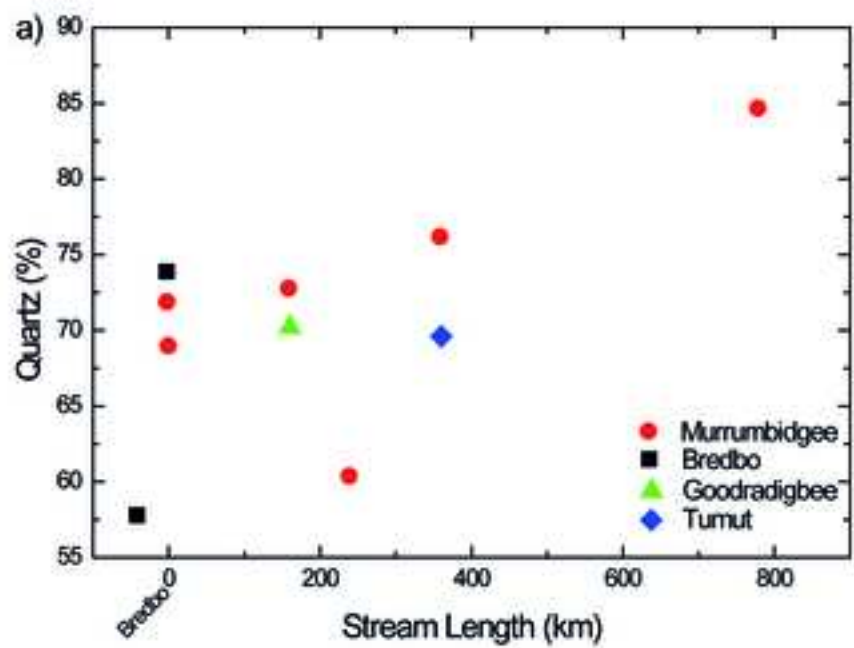


Figure 3  
[Click here to download high resolution image](#)

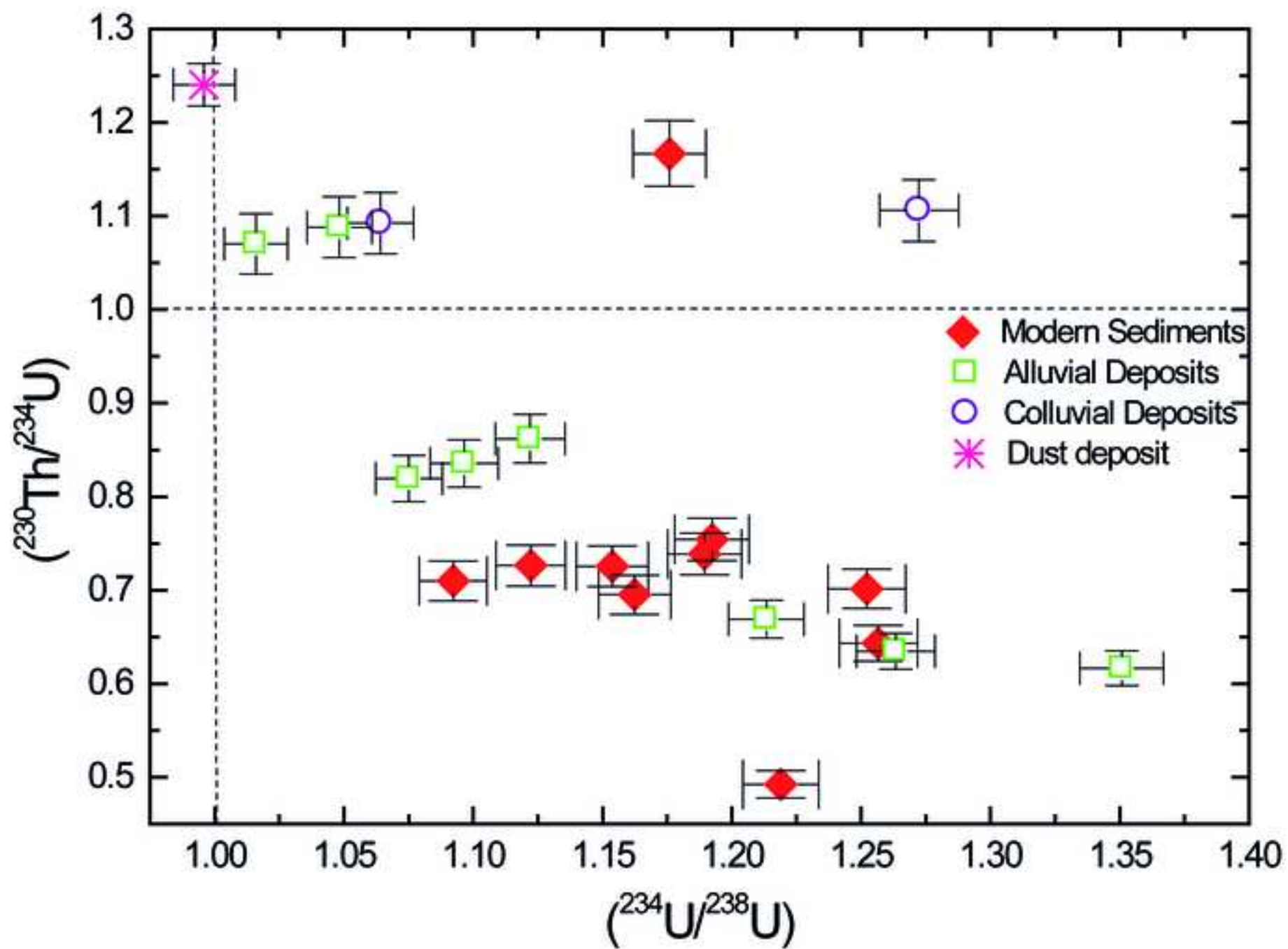


Figure 4  
[Click here to download high resolution image](#)

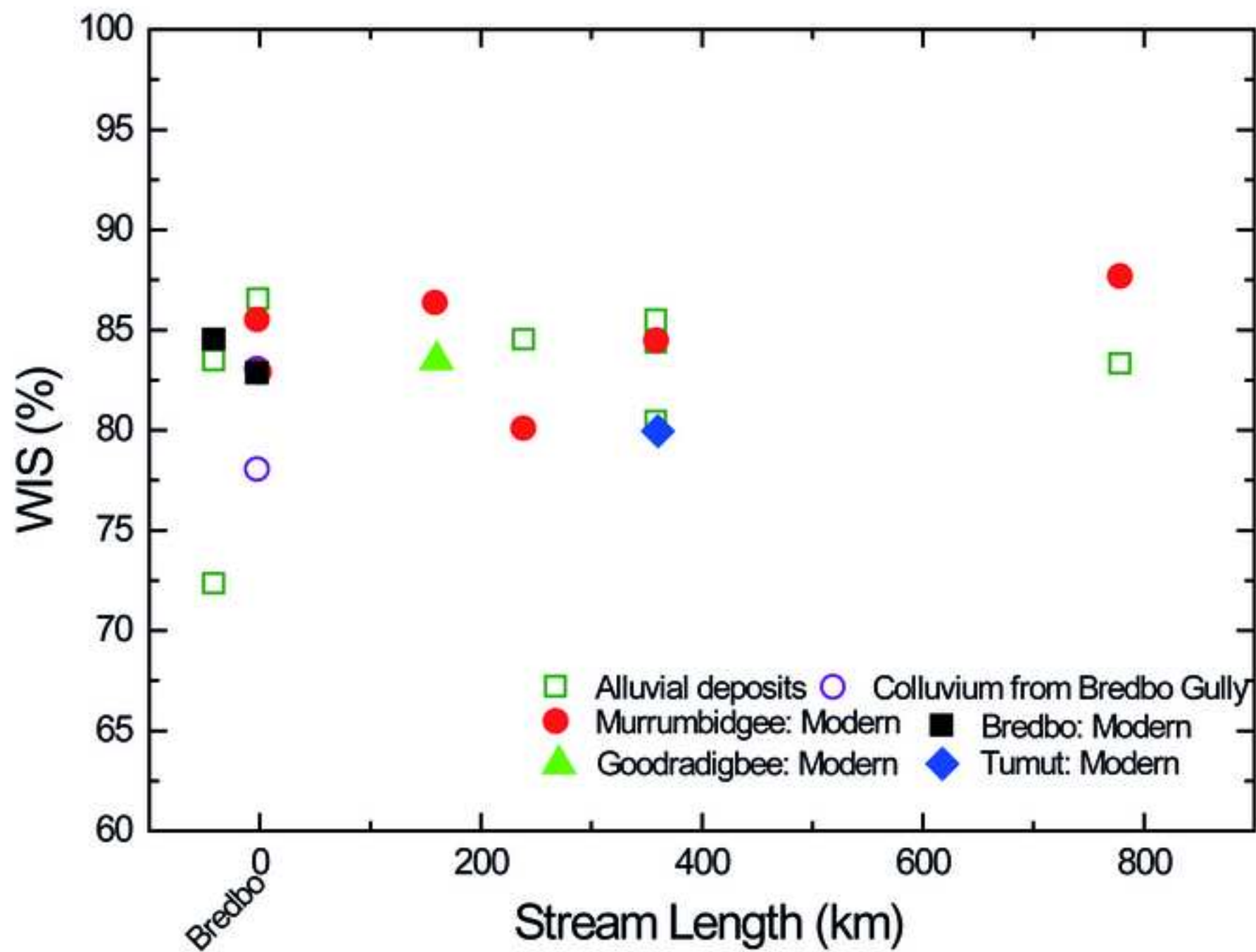




Figure 5  
[Click here to download high resolution image](#)

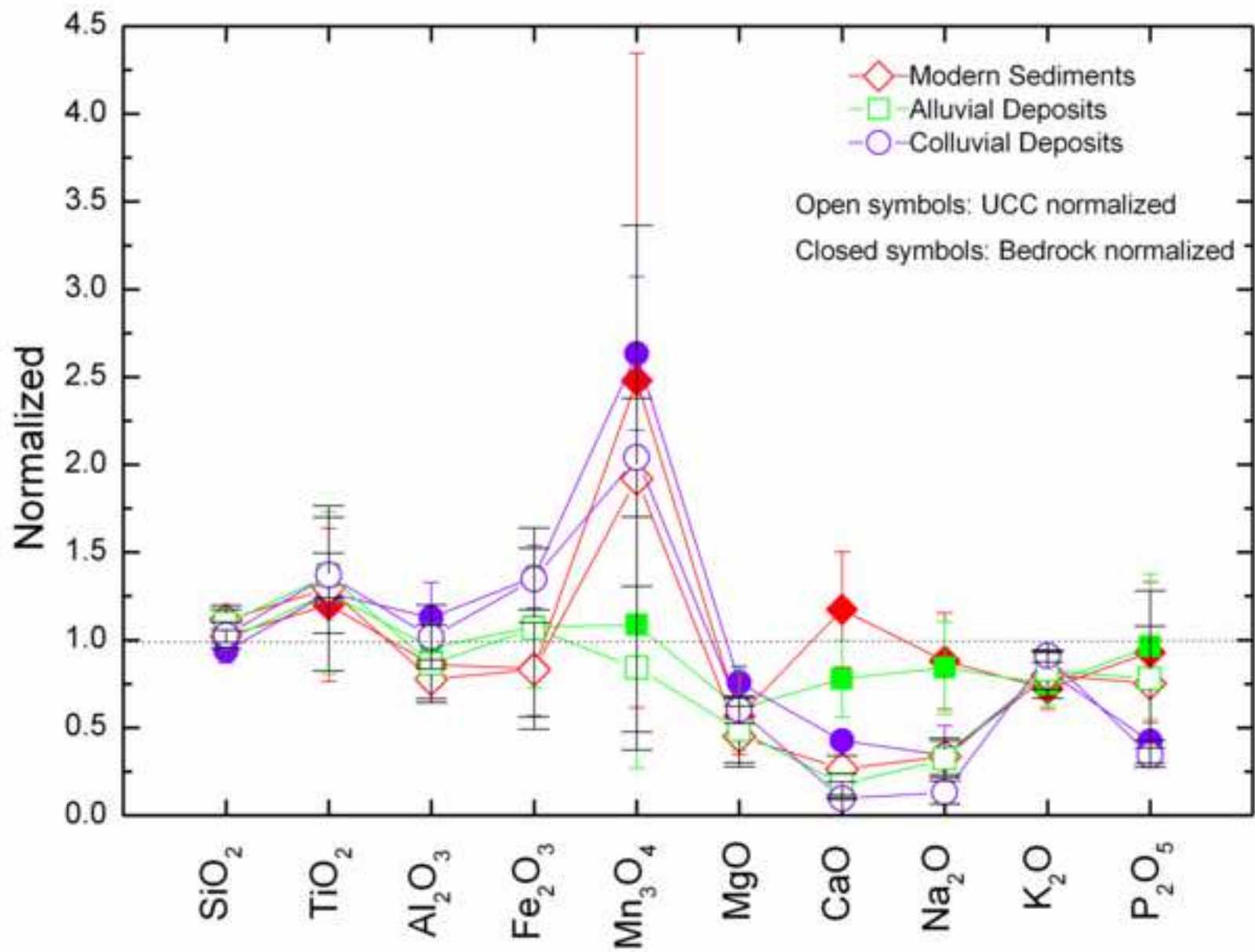


Figure 6  
[Click here to download high resolution image](#)

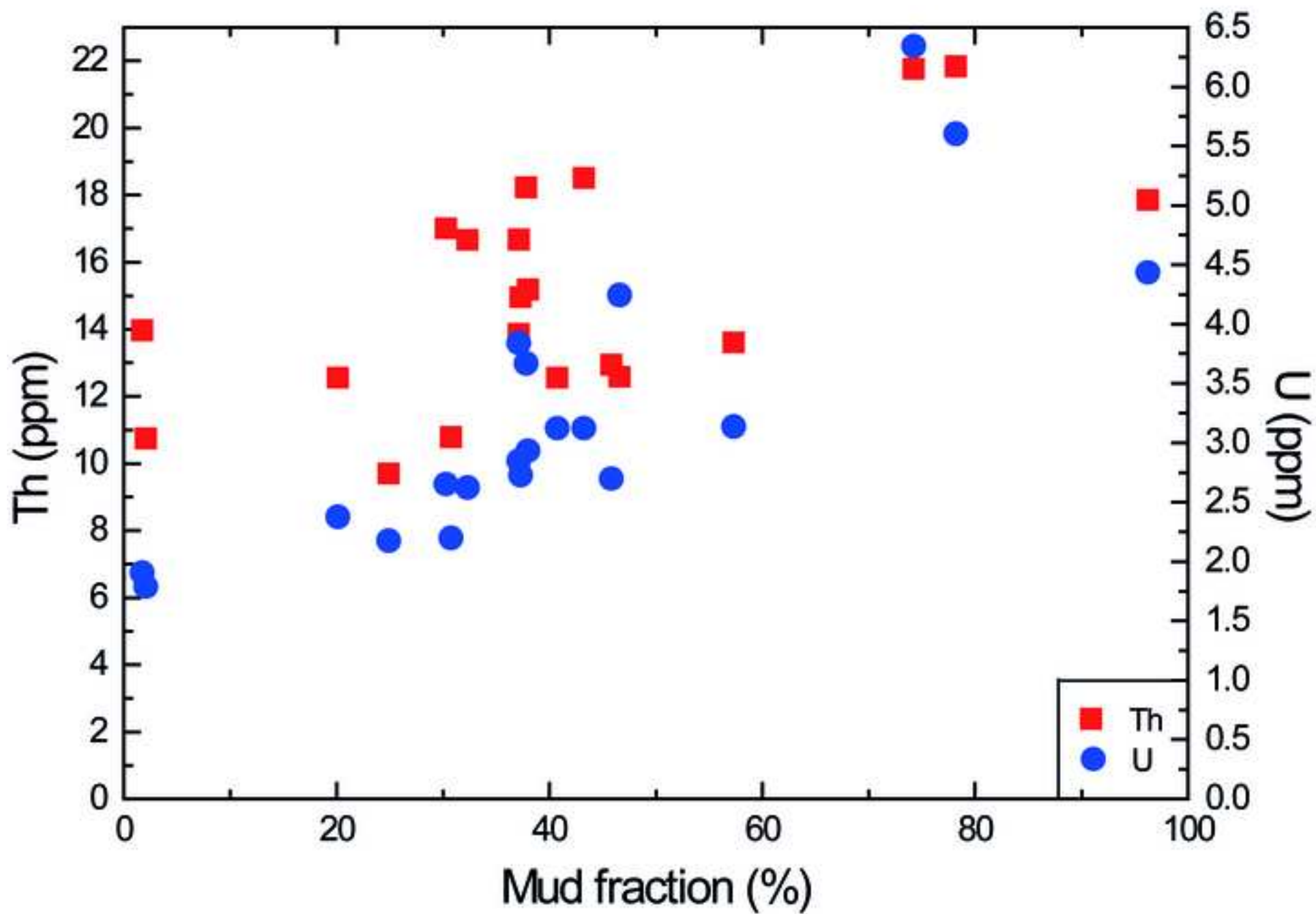


Figure 7  
[Click here to download high resolution image](#)

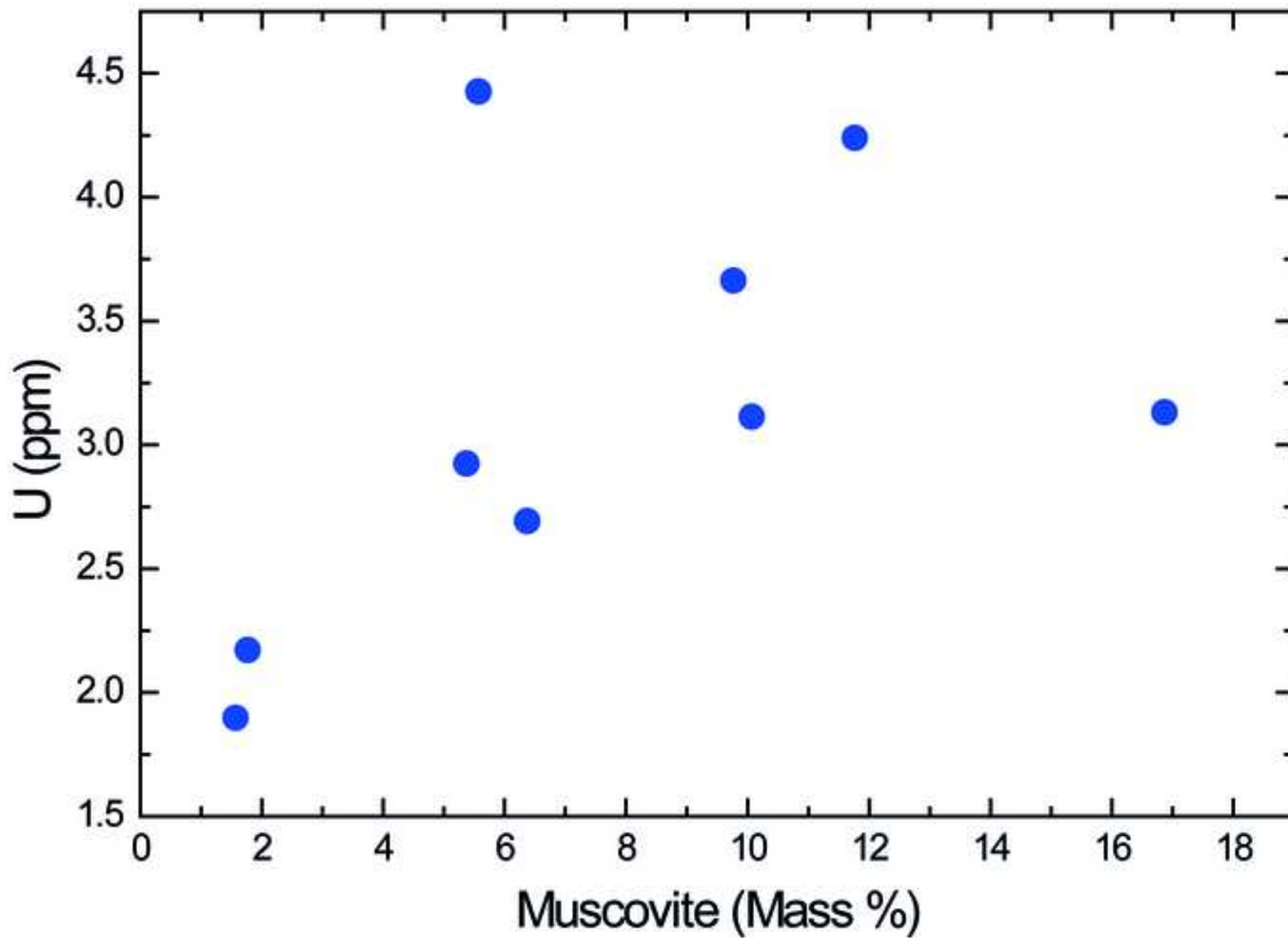


Figure 8  
[Click here to download high resolution image](#)

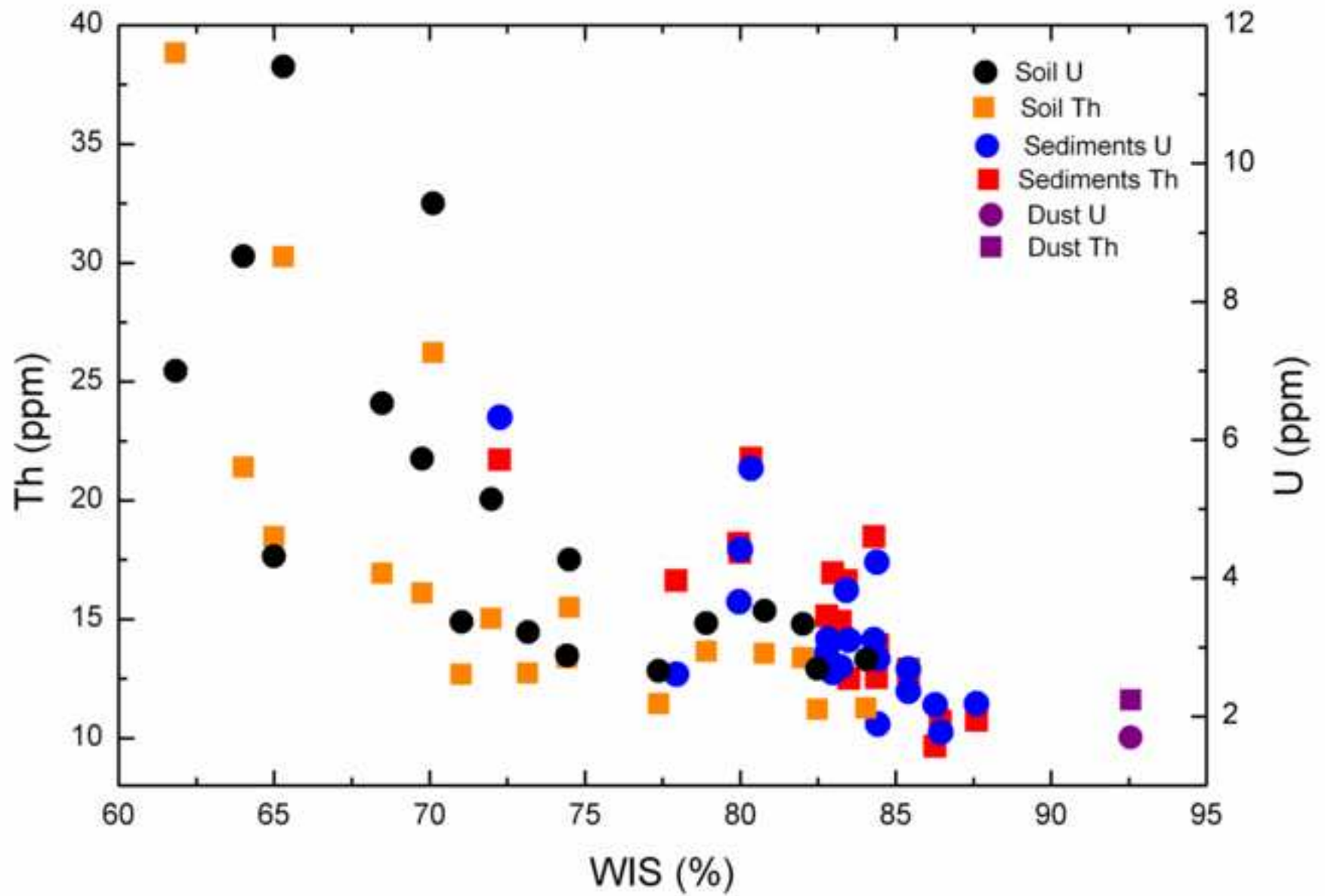




Figure 10  
[Click here to download high resolution image](#)

